

Article

Topographic Thresholds and Soil Preservation along the Southern High Plains Eastern Escarpment, Northwest Texas, USA

Travis Conley, Stance Hurst * and Eileen Johnson

Department of Biological Sciences, Museum of Texas Tech University, 3301 4th St, Lubbock, TX 79415, USA; trvscnly@gmail.com (T.C.); eileen.johnson@ttu.edu (E.J.)

* Correspondence: stance.hurst@ttu.edu

Received: 6 October 2020; Accepted: 18 November 2020; Published: 24 November 2020



Abstract: The eastern escarpment of the Southern High Plains (USA) is today a semi-arid erosional landscape delineated by canyon breaks and topographic relief. A series of buried soils were identified, described, and sampled at 19 soil profile localities exposed along terraces of the South Fork of the Double Mountain Fork of the Brazos River (South Fork) and two associated tributaries (Spring Creek and Macy 285 drainage). Radiocarbon dating revealed late-Pleistocene to early Holocene (~12,580–9100 ^{14}C B.P.), middle-Holocene (~6025–4600 ^{14}C B.P.), and late-Holocene (~2000–800 ^{14}C B.P.) buried soils. The late-Pleistocene to middle-Holocene soils were preserved only at higher elevations within the upper section of the South Fork and Spring Creek. A topographic position analysis was conducted using GIS to identify and examine the impacts of a soil topographic threshold on the preservation and distribution of buried soils within this geomorphic system. Above the identified ~810 m threshold, lateral migration of channels was constrained. Extensive channel migration below the threshold removed older terraces that were replaced with late-Holocene terraces and associated buried soils. Landscape topography constraints on geomorphic processes and soil formation impacted the preservation of archaeological sites in this semi-arid region.

Keywords: Southern High Plains; Texas; topographic threshold; GIS; grasslands; soils

1. Introduction

The threshold concept is commonly used for discerning the impact of geomorphic processes on landscape evolution [1–3]. Thresholds represent the point on the landscape in which the system of erosion or deposition changes [3]. Common threshold-based models involve the influences of topography [4] or erosion [1,5,6]. Topographic thresholds are typically identified through GIS analysis of digital elevation models DEMs [2,5]. How topographic thresholds effect gully formation, erosion, and stream dynamics has been of particular interest worldwide [7–9].

The use of thresholds to examine soil genesis, soil geomorphology, and the preservation of those soils across the landscape contributes to the understanding of the dynamics of landscape development and evolution [10–12]. Delineating thresholds across landscapes [13,14] provides a model for examining differences in soil formation processes, age of buried soils, and soil preservation. This landscape approach is particularly important in determining the relationship between buried soils and past hunter–gatherer occupations across the landscape [15,16].

Geomorphic systems are affected by thresholds. Geomorphic thresholds involve intrinsic and extrinsic aspects [17]. The geomorphic thresholds concept is one of abrupt landform change and that the landscape is not always in balance or equilibrium [17] (p. 93). The concept regards unstable landforms and that landform instability is inherent. Abrupt changes in erosion and deposition are part

of usual landscape development. Periods of instability are to be expected and can result from factors other than climatic change. Related to this concept are the concepts of complex response and episodic erosion [17] (pp. 486–487).

Similar to a geomorphic threshold, “a pedologic threshold is a limit of soil morphologic stability that is exceeded” by intrinsic change or extrinsic factors [18] (p. 100). Intrinsic change involves soil chemistry, mineralogy, or morphology whereas extrinsic factors are those involved in soil formation (climate, organisms, topography, and parent material [19,20]. As soil development occurs over time, the time factor is involved with threshold crossover in soil systems. Further, time scale is the main difference between geomorphic thresholds (shorter time scale) and pedologic thresholds (longer time scale), with pedologic ones involving times scales up to hundreds of thousands of years [18] (pp. 100, 106).

The relationship of pedogenic and geomorphic processes is a catenary one. Soil variability across a landscape is influenced by both sets of processes, resulting in catenas [20]. A catena is an outcome of the complex interplay between slope and soil development, erosion, and water movement. Past catenary relationships are reflected in paleocatenas where buried soils are preserved [14] (p. 234). Catenas are stable or unstable based on slope processes and that condition is an important aspect in landscape evolution. Landscape position is key and multistoried buried soils in a lower slope position reflect an unstable catena involving one or more K cycles [14,20]. A K cycle covers a period of erosion, deposition, and soil development, i.e., from landscape instability to stability [21]. Buried soils represent earlier K cycles. This concept underscores the periodic nature of soils and landscapes in how landscapes change and develop through time [14,21].

This study examines the geographic distribution of late-Quaternary buried soils developed in common parent materials in the ecotonal area between the Southern High Plains and westernmost Rolling Plains near Post, Texas (USA). The current study builds upon an initial statement of soil development and landscape evolution [22], and is governed by the concepts of soil systems thresholds [18,23] and catenas [14,23]. The aims of this study are to: (1) identify whether a threshold impacts the formation and preservation of soils within the research area; and (2) develop a model that integrates the results of the initial study [22] and current study to provide a better understanding of regional geomorphic processes and their impact on landscape evolution and the archaeological record.

Results of this research provide insights into the role of topography in the exposure and differential preservation of Quaternary-age sediments across the landscape. For field researchers, topographic thresholds impact the exposure and preservation of sediments, and therefore, the frequency and distribution of archaeological sites from different time periods. It is essential for field researchers conducting surveys and data modeling to account for the impact of topographic thresholds in sampling bias.

Research Area

The Post research area (Figure 1) is situated locally at the physiographic boundary between the Southern High Plains and the Rolling Plains (Central Lowlands). The Southern High Plains is located in northwestern Texas and northeastern New Mexico, with the Rolling Plains immediate to the east (Figure 1). Escarpments along three sides define the Southern High Plains, while to the south, the region merges with the Edwards Plateau (Stockton Plateau portion) without an obvious break. The Southern High Plains is a flat, expansive plateau. Approximately 25,000 small lake basins (fresh-water playas) and 40 salinas (saline depressions with brackish water) are present on the upland surface [23]. Northwest to southeast trending river valleys (draws) are tributaries of the Red, Brazos, and Colorado rivers that flow through the Rolling Plains and into the Gulf of Mexico.

Headward erosion of the Southern High Plains’ eastern escarpment during the Pleistocene has differentially exposed Triassic-age mudstones, sandstones and conglomerates (Dockum Group) [24], and the gravels, aeolian sediments, and Caprock caliche layer that comprises the Miocene to Pliocene-age Ogallala Formation within the research area [25,26]. In contrast to the flat Southern High Plains,

below the eastern escarpment, the breaks are rough, broken land formed from incision and erosion of the differentially resistant Ogallala Formation sediments and Triassic sandstone bedrock [24,27]. In the research area, the breaks are drained by numerous tributaries of the upper Brazos River basin.

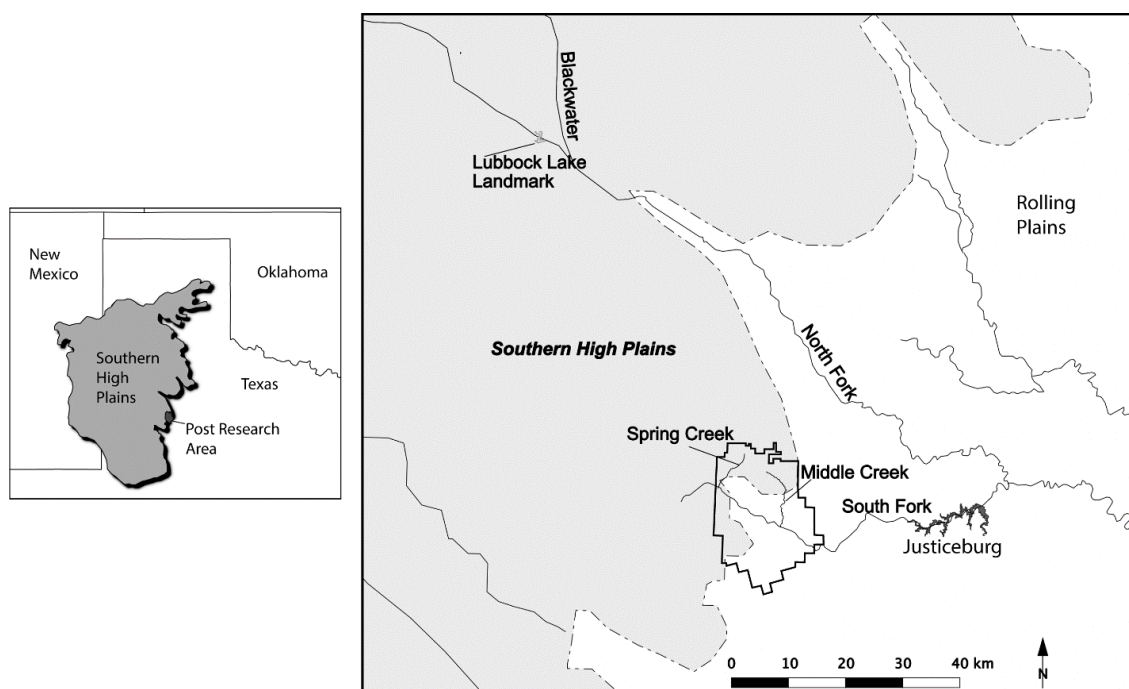


Figure 1. The Southern High Plains in northwestern Texas and eastern New Mexico (USA), highlighting the Post research area along the eastern escarpment into the westernmost Rolling Plains of Texas.

The Post research area consists of ~335 km² of ranchland that encompasses portions of the Southern High Plains uplands, escarpment breaks, and westernmost Rolling Plains. The modern climate is continental and semi-arid. Precipitation varies greatly on an annual basis, ranging from 130 mm to 1010 mm, but with a mean annual precipitation of 480 mm. Precipitation occurs mainly as spring and summer thunderstorms producing short episodes of heavy rain that can cause extensive erosion [28,29]. Groundwater springs emanating from the escarpment breaks remain a constant source of water feeding the tributaries [30].

The South Fork of the Double Mountain Fork of the Brazos River (hereafter South Fork) flows from northwest to southeast through the research area (Figure 2) with numerous spring-fed tributaries. These tributaries provide the main discharge of water and contribute to the formation of the landscape. Exposure of soils and stratigraphy occur throughout the upper South Fork basin. The current research focuses on a 16.18 km section of the South Fork and a 2.4 km long tributary of the South Fork (Macy 285 drainage) (Figure 2).

Past work in the research area examined a cross-section of buried soils from the Southern High Plains surface to the escarpment breaks [22]. Key results were: (1) late-Pleistocene to early Holocene (~11,000 to 8000 ¹⁴C B.P.) soils were exposed and occurred predictably at higher elevations near the escarpment and within inset terraces of reentrant valleys; (2) late-Pleistocene and early Holocene soils were absent at lower elevations away from the escarpment; and (3) intensive erosion had occurred during the middle Holocene that resulted in a period of net sediment removal, followed by net sediment storage with buried soils in low order drainages during the late Holocene. A late-Holocene series of soils (~2800 to 600 ¹⁴C B.P.) were exposed and predictable within inset terraces at lower elevations.

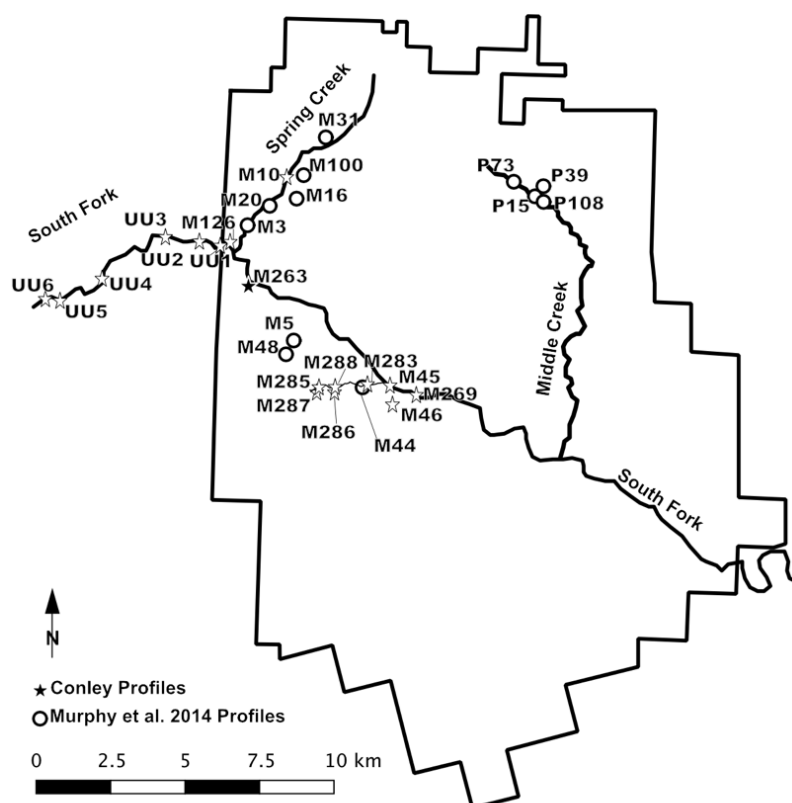


Figure 2. The Post research area and the location of soil profile localities from the current study (Conley profiles) and that of Murphy et al. (2014) along the South Fork River and its tributaries.

2. Materials and Methods

Field reconnaissance yielded 19 soil profile localities based on buried soils and sediments in alluvial parent materials and landscape positions. These localities were natural cut-bank exposures of terrace remnants associated with stream channels and floodplains of the South Fork and Macy 285 drainage. Soils were described and sampled using standard soil survey methods [31,32]. Pedon descriptions were recorded to indicate soil morphology and characterize soil properties. They were documented from the surface to the bottom of the Quaternary-age deposit, or until no dateable material was left to relate the age of the landform.

2.1. Soil and Sediment Analysis

A combination of particle size, calcium carbonate equivalence (CCE), total organic carbon content (OCC), and thin-section analyses were conducted at 16 of the 19 profiles to confirm field descriptions and to delineate episodes of parent material deposition.

Particle size descriptions were determined by sieving and the pipette method (NRCS method 3A1a1; [31,32]). Samples were pretreated to remove organic matter, and then dispersed in solution. Sand fractions (2–0.05 mm) were separated by wet sieving and dry sieving into their respective sand size classes: very coarse (2–1 mm); coarse (1–0.5); medium (0.5–0.25 mm); fine (.25–0.125 mm); and very fine (0.125–0.05 mm) [26]. Coarse fragments (>2 mm) were reported by a visual volume estimate determined in the field. Total sand fraction (0.05–2.0 mm) was used to analyze soil stratigraphy in order to eliminate the influence of translocated clay during pedogenesis.

The CCE has been determined using a total modified pressure method outlined by Soil Survey Staff [33] adapted by Clark and Hudnall [34]. The method has been modified to prevent the oxidation of organic matter and ensure complete digestion of calcium carbonate, limestones, and dolomites.

This method utilizes a Tensimeter to measure the pressure generated in a sealed container as a result of a reaction of the carbonates present in soil with hydrochloric acid (HCl). The reaction that takes place is:



The OCC is determined by the loss on ignition method [33]. Loss on ignition is a taxonomic criterion for organic soil materials [33]. Additional laboratory analysis of total carbon and total nitrogen has been determined by a LECO truspec CN analyzer.

2.2. Thin-Section Analysis

Samples were prepared for the petrographic microscope ensuring that intact pedes were impregnated with an epoxy without disturbing the soil fabric. The impregnated samples were cut into billets before being mounted onto a slide and ground to a thickness of 30 microns. The Geosciences Department at Texas Tech University performed the necessary preparations of the samples. The thin sections were examined using a Nikon Eclipse LV100POL polarizing light microscope equipped with a digital camera and monitor.

2.3. Radiocarbon Dating

Seventeen of the 19 localities have been sampled for radiocarbon dating, with 48 radiocarbon samples taken from the top and bottom 10 cm of each buried soil as feasible (Table 1). All of the samples were radiocarbon dated at the University of Arizona's AMS laboratory. Both residue and humate fractions have been dated for each sample. Dating both fractions limits the possibility for CaCO_3 contaminants, of particular importance in semi-arid regions, to obtain reliable results [30,31]. The reported age for each buried soil is the soil fraction yielding the oldest date as contamination by younger carbon is more likely than by older carbon [35–38]. When a fraction from a paired sample could not be dated, the dated fraction is reported but discounted as the older age could not be determined. Both uncalibrated radiocarbon years and calendar years are reported (Table 1). OxCal v4.2.3 using the IntCal 13 atmospheric curve (1 standard deviation) was used to calibrate radiocarbon ages to calendar.

2.4. Topographic Threshold Analysis

A topographic position analysis [39,40] was conducted to determine whether a soil system's topographic threshold was identifiable, what that threshold was, and its relationship to landscape position and the late-Quaternary stratigraphy across the study area. The deviation from mean elevation (DEV) raster calculation was used in this analysis as previous studies found it to be a more suitable measurement in heterogeneous landscapes [39]. The DEV "calculates the relative topographic position of the central point (z0), as the difference from the mean elevation divided by the standard deviation of the elevation, within a predetermined neighborhood (R)" [40] (p. 3438). Neighborhood focal statistics were used to create mean and standard deviation DEMs (digital elevation model) with a search radius of 300, 600, and 1200 m. Experimentation with different search radii was important to determine which neighborhood search radius was most appropriate for this analysis [40] (p. 3438). A DEM with 5 m resolution and Grass GIS 7.0 were used in these calculations. Results then were classified into five large-scale landscape morphological classes (ridge > 1.00; upper slope 1.00 to 0.50; middle slope 0.50 to −0.50; lower slope −0.50 to −1.00; and valley < −1.00) from the DEV raster based on Weiss [41]. These values indicated relative topographic variation in the landscape. The distribution of landscape classes was examined to determine their relationship to the distribution of dated soils and to aid in identifying a topographic threshold. Each raster was then visualized in Grass GIS with the 3D module.

Table 1. Radiocarbon ages determined on soil organic matter for the study area, listed by locality.

Locality	Soil Horizon	Depth (cm)	Material Assayed ¹	¹⁴ C Age (yrs. B.P.) ²	δ ¹³ C	cal yr B.P. ²	Dating Type	Lab No.
<i>Macy Locality 45 Profile A</i>								
CPMACY45A-01	2Ab3 + ky	130–140	SOM (r)	840 ± 65	−17.6	911-835	Conventional	A15779
			SOM (h)	1135 ± 95	−17.9	1282-844	Conventional	A15779.1
CPMACY45A-02	2ABb3 + ky	145–155	SOM (r)	1200 ± 65	−17.6	1270-980	Conventional	A15780
			SOM (h)	1645 ± 105	−17.4	1812-1343	Conventional	A15780.1
CPMACY45A-03	2ABb3 + ky	165–177	SOM (r)	1505 ± 70	−16.7	1537-1297	Conventional	A15781
			SOM (h)	1665 ± 115	−17.0	1860-1827	Conventional	A15781.1
<i>Macy Locality 45 Profile B</i>								
CPMACY45B-01	Ab1	63–76	SOM (r)	765 ± 80	−17.9	850-832	Conventional	A15782
			SOM (h)	730 ± 110/105	−18.4	906-831	Conventional	A15782.1
CPMACY45B-02	ABb1	76–90	SOM (r)	1070 ± 80	−17.6	1180-796	Conventional	A15783
			SOM (h)	975 ± 115	−18.7	1173-1159	Conventional	A15783.1
CPMACY45B-03	ABb1	90–106	SOM (r)	605 ± 75	−18.4	676-515	Conventional	A15784
			SOM (h)	800 ± 110	−19.1	932-624	Conventional	A15784.1
<i>Macy Locality 46 Profile A</i>								
CPMACY46A-01	2ABtkb	41–58	SOM (r)	920 ± 50	−15.5	928-736	Conventional	A15785
			SOM (h)	625 ± 135/130	−17.2	902-865	Conventional	A15785.1
<i>Macy Locality 126 Profile B</i>								
CPMACY126B-01	2ABk1b2	127–137	SOM (r)	1240 ± 70/65	−17.5	1293-1050	Conventional	A15801
			SOM (h)	1350 ± 55	−18.5	1367-1176	AMS	A15801.1
CPMACY126B-02	2ABk2b2	143–153	SOM (r)	1540 ± 55	−16.6	1546-1328	Conventional	A15802
			SOM (h)	1500 ± 35	−18.7	1520-1458	AMS	A15802.1
CPMACY126B-03	2AKb3	198–208	SOM (r)	1970 ± 55	−15.8	2108-2082	Conventional	A15803
			SOM (h)	2020 ± 35	−18.7	2102-2089	AMS	A15803.1
CPMACY126B-04	2ABkb4	292–302	SOM (r)	2685 ± 105/100	−19.2	3067-2676	Conventional	A15804
			SOM (h)	Insufficient Sample				A15804.1
<i>Macy Locality 263 Profile A</i>								
CPMACY263A-01	2ABb1	40–50	SOM (r)	Post-Bomb, 101.5 ± −0.9 pMC	−17.2		Conventional	A15805
			SOM (h)	220 ± 35	−16.6	421-410	AMS	15805.1
CPMACY263A-02	2Ab2	112–125	SOM (r)	930 ± 45	−15.0	929-744	Conventional	A15806
			SOM (h)	1060 ± 35	−16.4	1056-1021	AMS	A15806.1
CPMACY263A-03	2Ab3	162–173	SOM (r)	1755 ± 75/70	−17.6	1863-1844	Conventional	A15807
			SOM (h)	1740 ± 35	−17.7	1728-1557	AMS	A15807.1
<i>Macy Locality 269 Profile A</i>								
CPMACY269A-01	2Ab2	59–68	SOM (r)	720 ± 45	−15.0	733-635	Conventional	A15808
			SOM (h)	740 ± 35	−15.3	732-654	AMS	A15808.1

Table 1. Cont.

Locality	Soil Horizon	Depth (cm)	Material Assayed ¹	¹⁴ C Age (yrs. B.P.) ²	δ ¹³ C	cal yr B.P. ²	Dating Type	Lab No.
<i>Macy Locality 283, Profile A</i> CPMACY283A-02	2Ab1	74–82	SOM (h)	1335 ± 110	−15.6	1518–1490	Conventional	A15814.1
			SOM (r)	970 ± 55	−15.2	971–760	Conventional	A15815
			SOM (h)	1225 ± 130	−15.8	1390–911	Conventional	A15815.1
<i>Macy Locality 285 Profile A</i> CPMACY285A-01	2Akb1	82–92	SOM (r)	870 ± 45	−16.8	910–841	Conventional	A15816
			SOM (h)	960 ± 35	−21.0	933–792	AMS	A15816.1
	2Akb2	133–143	SOM (r)	1260 ± 35	−16.3	1283–1160	Conventional	A15817
			SOM (h)	1345 ± 35	−18.5	1315–1227	AMS	A15817.1
	2Ab3	193–203	SOM (r)	2355 ± 55	−16.6	2699–2632	Conventional	A15818
			SOM (h)	2255 ± 40	−17.3	2348–2292	AMS	A15818.1
	2ABkb4	235–245	SOM (r)	2825 ± 75	−16.5	3156–3089	Conventional	A15819
			SOM (h)	2715 ± 40	−18.1	2918–2912	AMS	A15819.1
<i>Macy Locality 286 Profile A</i> CPMACY286A-01	Akb1	33–50	SOM (r)	545 ± 45	−16.5	647–585	Conventional	A15820
			SOM (h)	640 ± 105/100	−14.6	785–499	Conventional	A15820.1
	2Akb2	82–95	SOM (r)	1105 ± 45	−15.7	1237–1206	Conventional	A15821
			SOM (h)	1305 ± 105/100	−16.6	1395–980	Conventional	A15821.1
	2Akb2	95–108	SOM (r)	1295 ± 50	−16.3	1302–1172	Conventional	A15822
			SOM (h)	1580 ± 105	−17.0	1705–1299	Conventional	A15822.1
	2Akb2	108–121	SOM (r)	1455 ± 65	−16.2	1523–1452	Conventional	A15823
			SOM (h)	1660 ± 105	−16.8	1817–1353	Conventional	A15823.1
<i>Macy Locality 286 Profile B</i> CPMACY286B-01	3Akb3	111–123	SOM (r)	1125 ± 55	−16.1	1176–936	Conventional	A15824
			SOM (h)	1205 ± 40	−17.3	1262–1052	AMS	A15824.1
	3ABssb4	145–155	SOM (r)	1365 ± 70	−16.0	1409–1172	Conventional	A15825
			SOM (h)	1195 ± 140/135	−17.0	1363–896	Conventional	A15825.1
<i>Macy Locality 287 Profile A</i> CPMACY287A-01	2A2b1	35–49	SOM (r)	815 ± 60	−17.0	906–853	Conventional	A15826
			SOM (h)	1330 ± 35	−19.0	1305–1225	AMS	A15826.1
<i>U.U. Locality 2 Profile A</i> CPUU2A-01	Ab1	16–26	SOM (r)	800 ± 50	−16.6	895–874	Conventional	A16085
			SOM (h)	1010 ± 75	−16.0	1071–738	Conventional	A16085.1
	ABb1	37–47	SOM (r)	1195 ± 65	−16.3	1269–976	Conventional	A16086
			SOM (h)	1250 ± 110	−17.3	1347–954	Conventional	A16086.1
	ABkb2	83–93	SOM (r)	1605 ± 65	−17.5	1690–1671	Conventional	A16087

Table 1. Cont.

CPUU2A-04			SOM (h)	1775 ± 110/105	−17.7	1945-1476	Conventional	A16087.1
	ABkb2	100–110	SOM (r)	1990 ± 60	−16.3	2114-1821	Conventional	A16088
CPUU3A-01			SOM (h)	1845 ± 25	−16.7	1864-1842	AMS	A16088.1
	2ABkb2	84–94	SOM (r)	9290 ± 215/205	−17.0	1186-10,119	Conventional	A16089
CPUU3A-02			SOM (h)	5705 ± 25	−18.8	6560-6411	AMS	A16089.1
	2ABkb3	130–140	SOM (r)	11,580 ± 140/135	−16.6	13,719-13,148	Conventional	A16090
CPUU3A-03			SOM (h)	Insufficient Sample	A16090.1			
	2ABkb3	150–159	SOM (r)	11,375 ± 170	−15.5	13,559-12,870	Conventional	A16091
U.U. Locality 4 Profile A			SOM (h)	Insufficient Sample	A16091.1			
CPUU4A-01								
	2Ak1b	61–72	SOM (r)	4520 ± 120	−16.5	5569-5559	Conventional	A16096
CPUU4A-02			SOM (h)	4655 ± 25	−16.6	5466-5346	AMS	A16096.1
	2Ak1b	94–106	SOM (r)	10,480 ± 200/195	−16.2	12,745-11,696	Conventional	A16097
CPUU4A-03			SOM (h)	12,275 ± 255/250	−16.3	15,195-13,606	Conventional	A16097.1
	2ABkb1	106–118	SOM (r)	10,270 ± 210/205	−16.1	12,600-11,310	Conventional	A16098
CPUU4A-04			SOM (h)	12,120 ± 290/280	−16.5	15,128-13,439	Conventional	A16098.1
	2ABkb1	130–142	SOM (r)	11,335 ± 285/275	−17.3	13,752-12,707	Conventional	A16099
U.U. Locality 5 Profile A			SOM (h)	12,580 ± 45	−17.3	15,154-14,667	AMS	A16099.1
CPUU5A-01								
	2ABkb1	29–39	SOM (r)	600 ± 70	−14.8	671-519	Conventional	A16100
CPUU5A-02			SOM (h)	900 ± 170/165	−15.9	1180-620	Conventional	A16100.1
	2Ak1b	63–74	SOM (r)	1465 ± 90	−15.1	1556-1240	Conventional	A16101
CPUU5A-03			SOM (h)	1600 ± 145/140	−15.8	1864-1841	Conventional	A16101.1
	2Ak1b	74–86	SOM (r)	1890 ± 80	−15.6	2001-1617	Conventional	A16102
CUU5-01			SOM (h)	2015 ± 30	−16.0	2044-1889	Conventional	A16102.1
CPUU5A-04	2Bk2b2	85,144.9	Charcoal	2210 ± 40	−22.9	2331-2133	AMS	A16079
U.U. Locality 6 Profile A	2Bk2b2	131	Charcoal	2340 ± 45	−21.7		AMS	A16080
CPUU6A-01								
	2ABk1b1	65–75	SOM (r)	3095 ± 100	−16.7	3557-3531	Conventional	A16103
CPUU6A-02			SOM (h)	5305 ± 185/180	−17.5	6447-5658	Conventional	A16103.1
	2ABk1b1	75–85	SOM (r)	4115 ± 100	−16.8	4865-4406	Conventional	A16104
CPUU6A-03			SOM (h)	6515 ± 250/240	−17.6	7927-7896	Conventional	A16104.1
	2ABk3b1	124–136	SOM (r)	8155 ± 230/220	−17.0	9547-8516	Conventional	A16105
CPUU6A-04			SOM (h)	9255 ± 240/235	−17.1	11,195-9886	Conventional	A16105.1
	2Ak1b	136–146	SOM (r)	9100 ± 205/200	−17.5	11,046-11,040	Conventional	A16106
CPUU6A-05			SOM (h)	8770 ± 250/240	−16.7	10,509-9283	Conventional	A16106.1
	2Ak1b	154–164	SOM (r)	9745 ± 200	−16.2	11,933-11,889	Conventional	A16107
			SOM (h)	9500 ± 260/250	−15.8	11,700-11,671	Conventional	A16107.1

¹ r = residue; h = humates; ² ± one standard deviation.

3. Results

3.1. Pedological Analysis

Radiocarbon results (Table 1) ranged from 12,580 to 800 ^{14}C B.P., with three soil forming periods reflected in the buried soils. The late-Pleistocene to early Holocene soils dated between $\sim 12,580$ and 9100 ^{14}C B.P. Middle-Holocene soils dated between ~ 6025 and 4600 ^{14}C B.P. The last soil forming period dated to the late Holocene between ~ 2000 and 800 ^{14}C B.P.

3.1.1. Late-Pleistocene to Early Holocene Soils

The oldest soil profiles are located in the upper portion of the South Fork (UU localities 3, 4, and 6; Figures 1–3 and Figures A1–A3). The informal name UU soil is used to identify a soil that formed between $\sim 12,580$ and 9100 ^{14}C B.P. The UU soil represents a time-transgressive surface and is a marker for the minimum age of late-Pleistocene- to early Holocene-age valley fill deposits. The range in stable carbon isotopes from radiocarbon assays (-15.5‰ to -17.5‰ ; Table 1) reflects a mixed grassland of C_3 and C_4 plant communities that formed under cooler and more moist conditions than today.



Figure 3. Late-Pleistocene- and early Holocene-age UU soil and middle-Holocene ULS soil (UU Locality 4) and accepted radiocarbon ages in a terrace remnant of the South Fork River within the eastern escarpment breaks of the Southern High Plains, Texas.

A fining upwards sequence in particle size indicated that the vertical accretion of alluvial sediments occurred slowly, keeping pace with the rate of pedogenesis. A relatively thick (~ 75 – 100 cm) organic-rich deposit with dark colors ($\sim 10\text{YR}/7.5\text{YR}3/3$) characterized the UU soil. Cumulic soil development in organic-rich sediments had a comparatively thick, buried mollic epipedon, with Stage I carbonate development. Visible secondary carbonates were identified throughout the UU soil. Depending on local conditions, these carbonates developed both pre-burial and post-burial. The distribution of carbonates throughout this buried soil suggested that soil welding had occurred.

Micromorphological analyses (Figure 4) of this soil show unconsolidated alluvium of predominantly Ogallala Formation sediments. Clastic textures of the sediments reveal a matrix supported, fine, moderately sorted, sub-rounded grains. Quartz is the dominant identifiable grain,

with feldspars, lithic fragments, and mica grains present in lower abundances. Lithic fragments, however, occur in a higher abundance than the other identified buried soils. Pedogenic fine-grained calcite occurs as ~8–12% of the total sample, and is identified generally as filling void spaces. Detrital carbonate grains show signs of weathering as evident by quartz inclusions and diffuse boundaries. Clay films are identified on grain surfaces. The clay films are oriented, but non-continuous, covering ~15–20% of grain surfaces. Clay films coat grain surfaces, with carbonate cement occurring after the development the clay films. Carbonates are identified mainly filling void spaces. Clay films generally do not occur where the majority of carbonates fill void spaces.

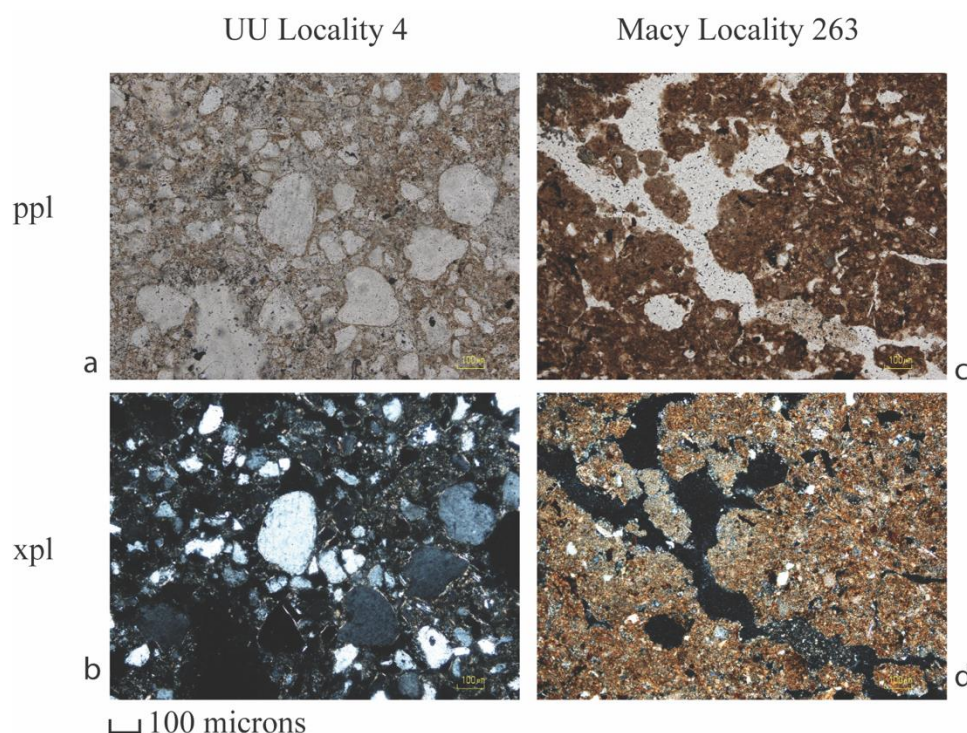


Figure 4. Petrographic images demonstrating micromorphological characteristics in the UU soil (UU Locality 4, photos (a,b)), and the late-Holocene pedocomplex of soils (Macy Locality 263, photos (c,d)) identified in the terrace remnants of the South Fork River within the eastern escarpment breaks of the Southern High Plains, Texas. (a) 10× magnification in plane polarized light. (b) 10× magnification in cross polarized light. (c) 10× magnification in plane polarized light. (d) 10× magnification in cross polarized light.

3.1.2. Middle-Holocene Soil

Middle-Holocene-age soils are documented in the upper section of Spring Creek (Macy Locality 10, Figure A4) at the confluence of Spring Creek and Macy Fork, and at two South Fork terrace localities (UU localities 4 and 6; Figures 2, 3, A2 and A3). ULS (U-Lazy-S) is used here as an informal name to correlate middle-Holocene soils across the research area. These middle-Holocene soils form at the end of alluvial sedimentation and were buried by colluvium or aeolian deposition. This truncated boundary suggests increased aridity after middle-Holocene pedogenesis. These soils range in age from ~6025 to 4600 ^{14}C B.P. (Table 1).

At the UU localities, the absence of clay films suggests an increase in drying during soil development. The presence of carbonates and their accumulation is derived from the aeolian sand deposited on top. Soil organic matter and stable isotope values (−16.6‰, −17.5‰, and −17.6‰) indicate that prior to burial, a middle-Holocene grassland environment was present over the landscape. That grassland has carbon contributions derived from both C_3 and C_4 plant communities.

Macy Locality 10 (Figure A4) represents a ponded alluvial deposit likely developed by slower flowing water. Clay films are present, and carbonate accumulations were secondary features from translocated carbonates. This situation suggests soil welding to some degree. Carbonate accumulation increases with depth, indicating a zone of illuviation associated with pre-burial. The carbon isotope values indicate C_4 vegetation populated the landscape.

3.1.3. Late-Holocene Soils

Soils and landscapes during the late Holocene develop through cumelic processes as denoted by the remaining 15 soil profile localities. These soils are expressed through a multistory or stacked vertical sequence (pedocomplex) rather than a singular buried soil (Figures 5 and A5, Figures A6–A16). Variations delimited at profile localities influence the number of buried soils and their characteristics during this formational period. Characteristics of the multistory sequence represent a marker for this period of landscape stabilization during the late Holocene and the soils that developed. The informal name of South Fork pedocomplex is used to correlate late-Holocene soils across the research area.



Figure 5. The late-Holocene South Fork pedocomplex (Macy Locality 263) and accepted radiocarbon ages of the South Fork River within the eastern escarpment breaks of the Southern High Plains, Texas; buried soils are identified with associated uncalibrated radiocarbon dates.

The Macy 285 drainage soil profile localities (Figure 2) provide a transect through sloping landforms leading to the main South Fork channel. As no discernable differences in sediment characteristics or timing of soil formation were identified, the Macy 285 drainage and lower South Fork terraces are grouped together.

A major soil forming period occurred from ~2000 to 800 ^{14}C B.P. The valley surface was abandoned as a frequently active alluvial depositional environment around ~800–600 ^{14}C B.P., then buried by

aeolian and slopewash sediments that blanket the entire landscape. The range in stable carbon isotopes from radiocarbon assays (-14.6‰ to -21.0‰ ; Table 1) reflected a mixed grassland of C_3 and C_4 plant communities.

Similar pedogenic features are common through these late-Holocene sediments. The buried soils are in alluvial sediments distinguished by fining upwards sequences that express lateral variation of overbank deposition. Soils generally exhibit cumulic soil development through vertical accretion of sediments that kept pace with the rate of pedogenesis. Higher values of organic matter, with darker colors ($\sim 10\text{YR}/7.5\text{YR } 3/3$), characterize the soils in the pedocomplex. Localized conditions determine the amount of organic matter input from vegetation, and soil horizons are either mollic or ochric epipedons. Visible secondary carbonates are identified as soft masses and root tracings throughout these soils, with Stage I carbonate development. Carbonates have developed both pre-burial and post-burial, with variation of intensities determined by local conditions. The distribution of carbonates through the pedocomplex suggests that soil welding had occurred.

Micromorphological analysis (Figure 4) shows these late-Holocene soils are composed of an unconsolidated mix of alluvium from Ogallala Formation and Triassic sediments. Clastic textures of the sediments reveal matrix supported, very fine, well-sorted, rounded grains. Quartz is the dominant identifiable mineral grain, with feldspars, lithic fragments, and mica grains present in smaller abundances. Pedogenic fine-grained calcite is relatively non-existent. Detrital carbonate grains, however, are more prevalent when compared to the older late-Pleistocene and early Holocene sediments. These detrital carbonate grains do not show a high degree of weathering, demonstrating relatively high relief and sharp boundaries. Occasionally, detrital carbonate grains show signs of weathering as evident by quartz inclusions, however, it is not known if the degree of weather occurred post-deposition. Clay films occur on $\sim 5\text{--}15\%$ of the grains, evident on grain surfaces. The clay films are oriented, but non-continuous covering $\sim 10\text{--}15\%$ of grain surfaces. The clay matrix of these late-Holocene-age sediments contains a much higher amount of iron oxide clays, representing sediments sourced with more inputs from reworked Triassic alluvial sediments.

3.2. Radiocarbon Dating

The radiocarbon ages for most of the profiles are in chronological order from top to bottom (Table 1). Only five dates are out of sequence, and of those, only two were from separate soil horizons [UU Locality 4 Profile A (CPUU4A-02, 03) and UU Locality 6 Profile A (CPUU6A-03, 04), Table 1]. The other three are from the same soil horizon sampled within 10 cm of each other [Macy Locality 45 Profile B (CPMACY45B-02, 03), Macy Locality 283 (CPMACY283A-01, 02), and UU Locality 3 Profile A (CPUU3A-02, 03)]. In addition, only at Macy Locality 45 Profile B do out-of-sequence radiocarbon ages not overlap within their error ranges ($A15783, 1070 \pm 80 \text{ }^{14}\text{C}$; $A15784, 1800 \pm 110 \text{ }^{14}\text{C B.P.}$, Table 1). Overlap in most of the out-of-sequence radiocarbon ages suggests continuous pedogenesis during the time-frame to produce overlapping radiocarbon ages within a 20 cm vertical span.

The younger of the out-of-sequence dates at Macy Locality 45 Profile B ($A15784.1, 800 \pm 110 \text{ }^{14}\text{C B.P.}$, Table 1), UU Locality 4 Profile A ($A16098.1, 12,120 \pm 290/280 \text{ }^{14}\text{C B.P.}$, Table 1), and UU Locality 6 Profile A ($A16106, 9100 \pm 205/200 \text{ }^{14}\text{C B.P.}$, Table 1) are discounted because they are younger in age than the dates immediately above them. It is more difficult to introduce older materials to bias the results in comparison to more recent sources of carbon contamination [35].

3.3. Topographic Position Analysis

The differences in the neighborhood search radii (300, 600, and 1200 m) used in the analysis had a big impact in landscape classification (Figure 6). At 300 m, much of the Southern High Plains surface was classified as middle slope. This scale, then, masked an overall pattern in landscape classification and was not used. Patterns in landscape classification at 600 m became apparent and more so at 1200 m. These two search radii were used in the analysis.

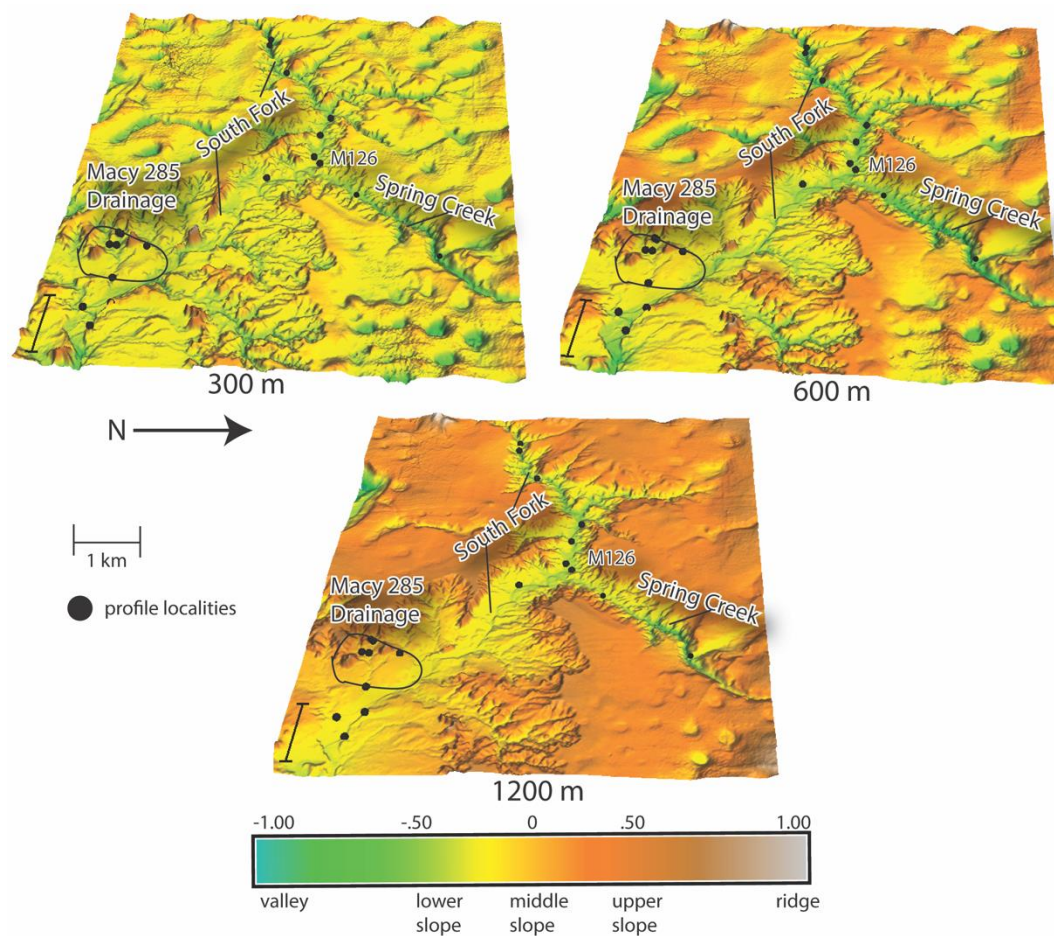


Figure 6. Maps generated classifying landscapes using differing neighborhood search radii (300, 600, and 1200 m) for the South Fork drainage in the eastern escarpment breaks of the Southern High Plains, Texas.

At 1200 m, the part of the landscape classified as valley, i.e., within the South Fork and Spring Creek axes, was concentrated within the escarpment breaks and at higher elevations (Figure 6). At lower elevations away from the breaks along the South Fork axis, the valley classification ceases and instead the South Fork is classified as lower slope. All buried soil profile localities along the South Fork and Spring Creek were classified within the valley class at 600 m. At 1200 m, however, only buried soil profiles at Macy Locality 126 and higher elevations were within the valley classification along the South Fork and Spring Creek axes. Both the 600 m and 1200 m search radius placed the buried soil profiles within the Macy 285 drainage (Figure 6) within the lower to middle slope classes.

The topographic threshold at which the topography impacted the valley landscape classification is at an elevation of ~810 m between the UU2 and UU3 localities above where Spring Creek meets the South Fork (Figure 7). The slope gradient within the South Fork changes from 0.577 above the topographic threshold to 0.385 below this threshold. The continued valley classification of the South Fork above the ~810 m threshold indicates a higher degree of topographic relief and confined vertical channel incision that typifies the escarpment breaks. Moving down valley at lower elevations, the South Fork channel becomes less confined with more lateral movement. The late-Pleistocene to middle-Holocene soils are found only above this ~810 m threshold associated with the 1200 m search radius valley classification. These older buried soils have a much better chance of preservation with less lateral movement of the South Fork above the ~810 m threshold.

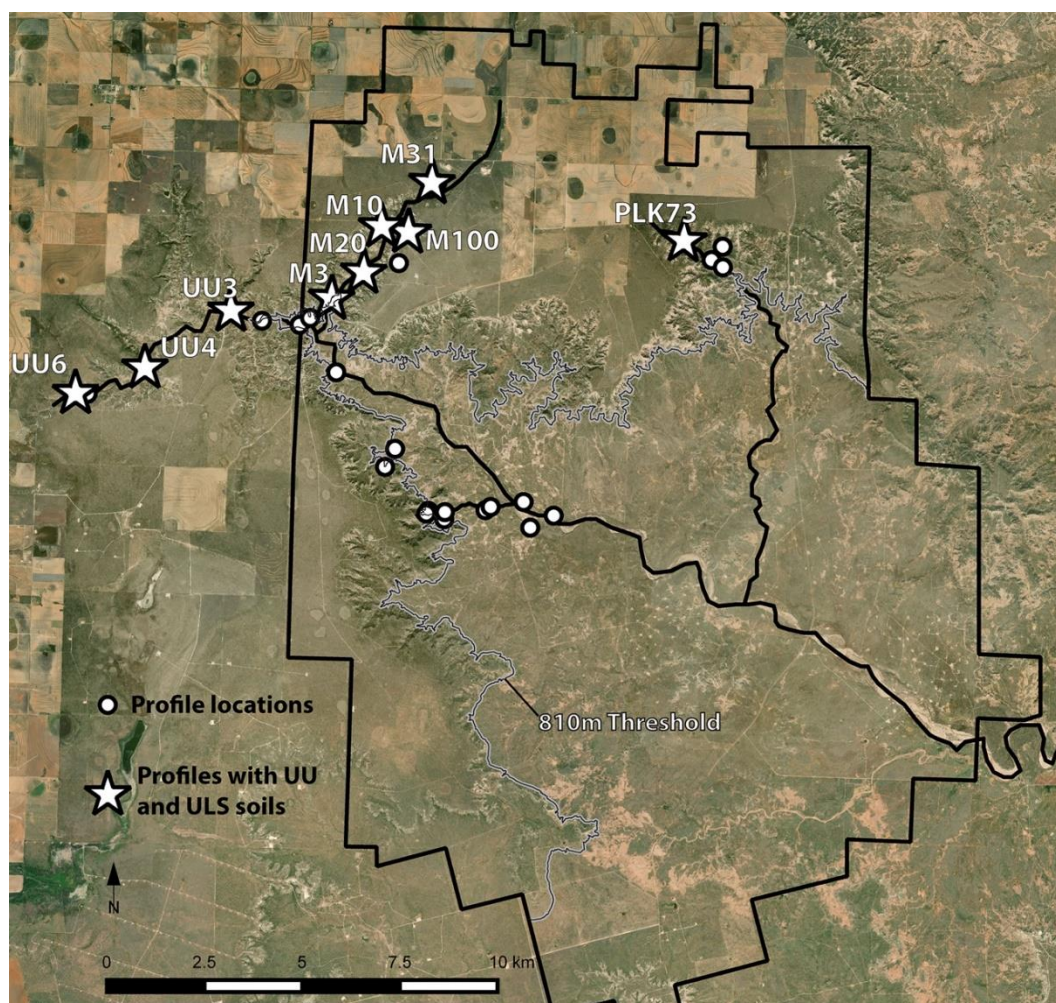


Figure 7. Location of soil profile localities from the current study and that of Murphy et al. (2014) in relation to the ~810 m threshold at the Post research area along the eastern escarpment into the westernmost Rolling Plains of Texas.

4. Discussion

Based on soil stratigraphic records and radiocarbon ages, the alluvial terraces of the South Fork represented a transect through the study area. Nineteen profiles were examined to identify formational characteristics and the effect of topography on the distribution and preservation of buried soils in the divergent Southern High Plains eastern escarpment breaks. Profile localities of a singular buried soil indicated landscape stability persisting through time. Multistory profile localities provided a range of soil development periods separated by episodes of deposition and erosion (K cycle). Localized factors in soil formation determined the number and thicknesses of these buried soils. These soils, however, exhibited similar pedogenic characteristics that were differentiated by time.

Radiocarbon dating the buried soils produced a range of burial times from ~12,580 to 700 ^{14}C B.P. (Table 1). Most of the radiocarbon ages were within chronological order for each profile. Overlaps in radiocarbon age error ranges between samples collected within 20 cm of each other indicated continuous pedogenesis for many of the soil sequences.

Late-Holocene (~2000 to 800 ^{14}C B.P.; Table 1) buried soils were the most common and traceable across both the terraces of the South Fork and the Macy 285 drainage [42]. The predominance of late-Holocene sequences of buried soils also was well documented ~40 km downstream (near Justiceburg; Figure 1) in the westernmost region of the Rolling Plains [43]. In contrast, the UU-age soil (~12,580 to 9100 ^{14}C B.P.; Table 1) and ULS-age soil (~6025 to 4600 ^{14}C B.P.) were found in only four

of the 19 profiles. These profiles were all located in the upper reaches of the South Fork where the valley margin is much narrower.

The UU and ULS soils were found only above the ~810 m threshold (Figure 7). Results from the topographic position analysis found that above this threshold, the surface was classified as a valley, even with larger neighborhood search ranges. This situation indicated that above the threshold, the valley margin is well defined in comparison to below the threshold.

A late-Pleistocene and early Holocene soil (UU soil) developed through cumelic soil processes in the canyon-confined areas in the upper reaches of the South Fork drainage. These processes resulted in the development of a thick, organic-rich soil. Small quantities of alluvium were deposited slowly that allowed soil development to keep pace with alluviation.

A middle-Holocene soil (ULS soil) also is preserved above the threshold within upper South Fork and Spring Creek. These soils represent a period of stability before an erosional event marked by an erosional disconformity and then burial by aeolian or colluvial sediments.

In contrast, downstream morphology of the South Fork drainage revealed a late-Holocene series of multistoried buried soils or a catena (the South Fork pedocomplex). The development of multistoried buried soils along this section of the South Fork channel and Macy 285 drainage was a product of fluctuating rates of alluviation. Accretionary sedimentation periodically slowed or completely ceased, resulting in the formation of a series of stable land surfaces during the late Holocene. These buried soils were composed from various inputs of reworked Ogallala Formation and Triassic sediments and showed less effects from weathering due to more recent deposition than the older UU and ULS soils ([42]; Figure 8). This catena formed a landscape-wide, late-Holocene pedocomplex.

The topographic positioning index defined valleys predominantly in the upper reaches of the South Fork. More valleys were classified through the neighborhood search radii. Increasing the radii (600 to 1200 m) produced a larger variance in elevations that provided an expanded classification of valley and lower slopes. A soil topographic threshold at ~810 m elevation was identified just above the confluence of the South Fork channel and Spring Creek drainage (i.e., moving downstream out of the canyon-confined area). It was at this point where the first initial outcroppings of the Triassic redbeds are exposed (Figure 7). Above this threshold, the valley channel was more confined by bedrock with less lateral movement from the South Fork in comparison to below the threshold when the valley begins to widen.

Sometime prior to ~13,000 ¹⁴C B.P., the upper reaches of the South Fork incised and created a terrace in which the UU and ULS soils formed. During the later Holocene, erosion removed the late-Pleistocene to Middle-Holocene-age terraces containing the UU and ULS soils below the threshold because of more lateral movement of the South Fork in its less confined valley setting. In contrast, above the threshold, the lack of or minimal lateral migration in the upper reaches preserved the soils and their terraces. That situation would explain why at 1200 m search radius, a valley classification occurs above ~810 m elevation but not below that elevation. The South Fork drainage valley axes above the ~810 m elevation threshold were more confined. This confinement was due to bedrock and a steeper gradient.

Topographic position analysis is a common technique used to subdivide landscapes into geomorphic classes for research [39] (p. 40). The advantage of this approach is that it provides an objective and replicative method to classify the landscape. The spatial relationship between landscape classes, derived from topographic position analysis, and the age of buried soils has been used to identify a soil threshold. Based on these results, the spatial areal extent of valley classification across the landscape has been used to identify the ~810 m threshold within the research area (Figure 7). The ~810 m threshold marks a crossover in pedogenesis from the canyon breaks to the lower lying South Fork Valley. Topography in this research represents a primary driving extrinsic factor in soil development effecting the matrix of parent material, and then soil burial and preservation.

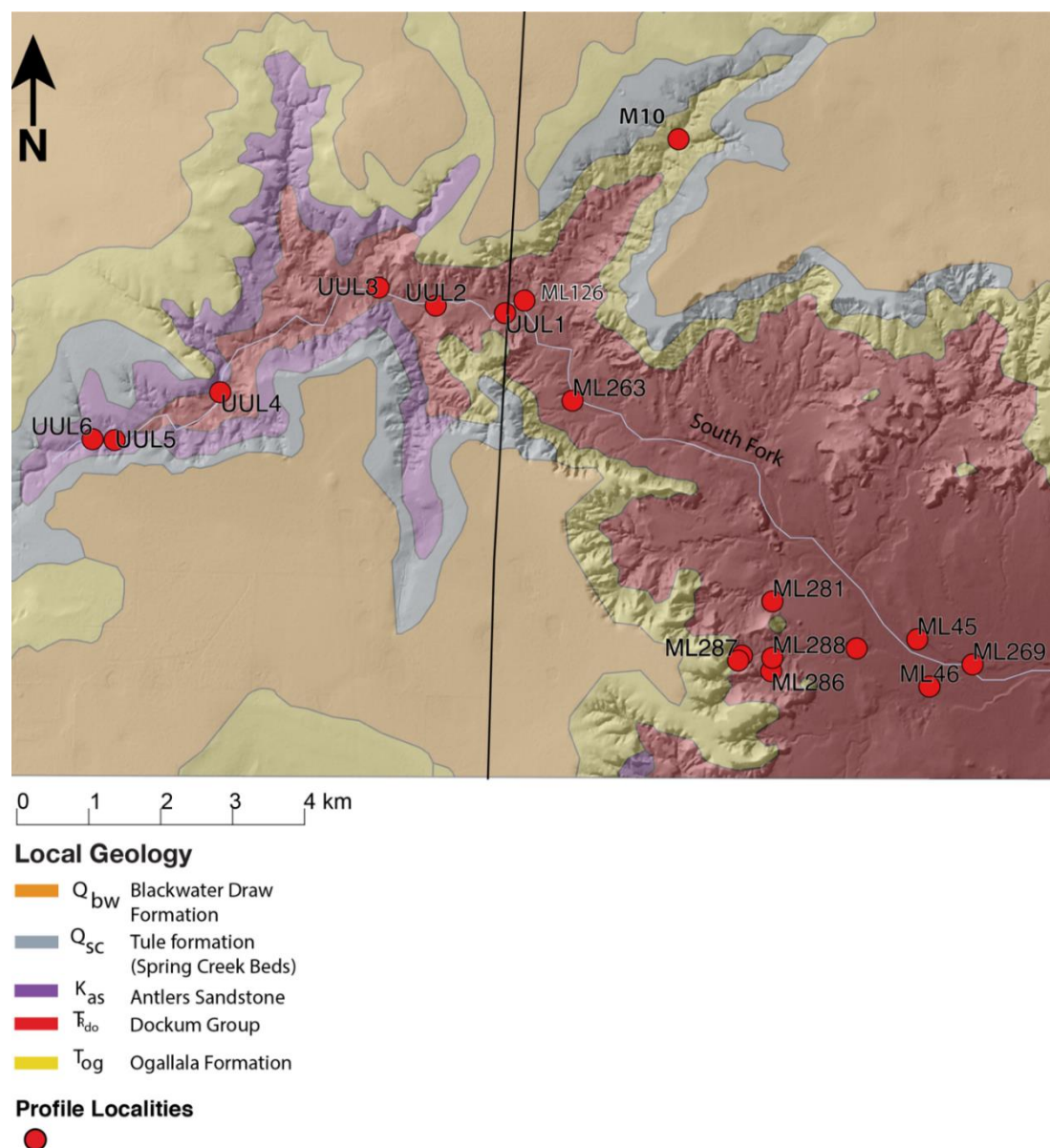


Figure 8. Geologic map with profile localities for the current study area in the eastern escarpment breaks of the Southern High Plains, Texas. Geologic source data derived from the Texas Geological Database (2014).

The Triassic redbeds highly influenced the South Fork's channel dynamics (Figure 8). The channel changed from highly incised and dissected landforms to broader floodplains with larger amounts of net sediment supply. In the lower portions of the South Fork channel further downstream, the topographic relief was less and resulted in landforms classified as middle and lower slopes. The late-Holocene catena dominated and transformed the landscape. The Macy 285 drainage was intended to provide a transect across the middle and lower slopes outside of the canyon-confined areas higher in the drainage network. Pedological and radiocarbon analyses, however, identified that buried soils in this drainage developed at the same time as landforms associated with the lower, broader channel of the South Fork. This situation further strengthened the topographic soil threshold as occurring upstream.

The general soil threshold model developed from this study indicates a crossover in pedogenesis or soil/landscape preservation at a certain elevation, with the late-Pleistocene to early Holocene soil and middle-Holocene ULS soil restricted to the upper reaches of the drainage system, and late-Holocene soils found in both the upper and lower reaches. The late-Holocene multistoried soils are documented

across the lower reaches. Topography drives the differential burial and preservation of the soils. This model is strengthened by the integration of a previous study adjacent to and slightly overlapping the current research area.

Murphy et al. [22] examined profiles along Spring Creek, Middle Creek, and smaller unnamed tributaries of the South Fork (Figures 2 and 7). Soils in the upper reach of Spring Creek dating to the early Holocene ranged in age from ~10,730 to 8155 ^{14}C B.P. (Figure 7). Late-Pleistocene lacustrine muds were dated from cores, the oldest ages being ~22,300 and ~15,000 ^{14}C B.P. Applying the threshold model, these soils and muds were found above the ~810 m threshold (Figure 7). Middle-Holocene soils documented in the upper reaches of Spring and Middle creeks ranged in age from ~6025–4600 ^{14}C B.P. These soils also were found only above the ~810 m threshold (Figure 7). Packages of late-Holocene-age sediments and soils were found both below and above the ~810 m threshold [22].

Integration of the two datasets demonstrates that the model holds for this segment of the escarpment—plains interface. Specific to this research area, the late-Pleistocene to early Holocene soils documented by Murphy et al. [22] are interpreted as the UU soil. In turn, their middle-Holocene soils are grouped as the ULS soil. It also is clear that the late-Holocene multistoried soils of Murphy et al. [22] are part of the South Fork pedocomplex. These informally named buried soil groupings express and are part of the soil threshold model, each reflecting soil threshold elevation, topographic position, and age.

An important threshold found in stream channels is the transition from upland valley to distal floodplain valleys [44] (p. 53). In upland valley settings, the adjacent hillslopes are coupled to the stream and sediment is removed directly from hillslopes and through the streams. The downstream floodplain below the threshold is decoupled from neighboring hillslopes and is a place of sediment accumulation within a broader floodplain setting.

A wide range of sediment sizes are poorly sorted within sediments in channels within the uplands above the threshold [44]. In contrast, below the threshold, smaller materials are moved downstream and the sediments are finer and well-sorted. In the Post study area, a transition occurs in sediment texture from fine and moderately sorted to very fine and well-sorted sediment matrix from the UU soil to the ULS soil to the late-Holocene soils of the South Fork pedocomplex. In addition, above the ~810 m threshold, the sediment matrix is dominated by Ogallala Formation sediments, while below the threshold, soils formed in a mixture of both Ogallala and Triassic sediments [42]. This situation further demonstrates that above the threshold, the channel sediments are coupled with the exposed Ogallala Formation sediments on the adjoining hillsides. Below the threshold where the valley broadens out, a change takes place where sediment storage is both Ogallala and Triassic material. This change indicates that the stream channel in this location is decoupled from the adjoining hillsides.

Archaeological surveys and excavation in the region since 2005 have identified over 350 localities ranging in age from Paleoindian ~11,000 ^{14}C B.P. to Anglo-American settlement of the region (AD ~1877–1950). Late-Holocene-age localities are recorded both above and below the threshold in the research area. For example, Macy Locality 126 is located at the confluence of Spring Creek and the South Fork below the threshold. Survey and excavation at this site have uncovered a multi-occupational Ceramic- to Protohistoric-age (700–400 ^{14}C B.P.) campsite locality [45]. Above the threshold, a Ceramic-age (~2000 to 1000 ^{14}C B.P.) occupation has been documented at Macy Locality 16 [46].

In contrast, Paleoindian to Middle-Archaic occupations have been documented mainly above the ~810 m threshold. Paleoindian research has focused on deposits exposed along Spring Creek located above the ~810 m threshold. To date, a Clovis projectile point (~11,000 ^{14}C B.P.) comes from the surface (Macy Locality 10), and excavation has revealed a Folsom-age (~10,400 ^{14}C B.P.) bison kill/processing feature (Macy Locality 349). In addition, a Middle-Archaic Bell projectile point (~6000 to ~5000 ^{14}C B.P.) found on survey at Macy Locality 10 likely is associated with the ULS soil documented at that locality. Research in Spring Creek also has focused on several Quaternary paleontological localities (e.g., Macy Locality 100) that have provided important insights into late-Pleistocene to early Holocene (~11,500–8000 ^{14}C B.P.) faunal communities [47,48].

Channel migration below the topographic threshold has altered the landscape and removed most Paleoindian to Middle Archaic-age deposits and left behind a late-Holocene record. Above the topographic threshold, constrained channel migration has preserved a Paleoindian- to Middle Archaic-age record. Exceptions are surface late-Paleoindian (~10,000–8600 ^{14}C B.P.) localities that have been found below the threshold. For example, at Macy Locality 15, a chalcedony Plainview point (~10,000 ^{14}C B.P.) associated with a few tools and a basal thinning flake have been recovered [49].

The eastern Southern High Plains escarpment [27], draws of the Southern High Plains [35], and stream valleys in the westernmost Rolling Plains [27,43] contain buried landscapes expressing the late Pleistocene through Holocene geoarchaeological record. A number of Southern Plains studies have identified and examined the lateral distribution of buried soils and past stable landscapes through time [27,43,50]. The Post research area, however, is different than many of the study areas identified on the adjoining Southern High Plains and Rolling Plains because the topographic influences are much higher in comparison. Within the escarpment breaks, spatial and temporal discontinuities reflect the evolution in these landscapes in response to natural formation processes. They generally relate to the conditions present in the regional environment. The escarpment breaks are defined by lateral erosion of the Southern High Plains, and erosion and downcutting by the headwaters of the South Fork. Due to the high topographic relief, the escarpment breaks are a source of sediment that supplies the South Fork.

In the adjacent Southern High Plains and Rolling Plain regions, the late-Pleistocene to middle-Holocene sediments are deeply buried within draws or along older terrace settings. In the research area, these early sediments and associated buried soils (i.e., UU soil and ULS soil), however, are exposed only in the upper reaches within the escarpment breaks. Along the South Fork ~40 km downstream from the Post research area, late-Pleistocene through middle-Holocene soils are preserved only in the higher elevations of tributaries feeding into the South Fork (Figure 1). In addition, terraces of late-Holocene age along the South Fork are well preserved and laterally traceable [43].

The regional soils record of the Southern High Plains eastern escarpment and the westernmost Rolling Plains, then, indicates climate change, with a shift from the cooler and humid late Pleistocene to the arid and semi-arid conditions of the middle and late Holocene. This shift has caused the stripping of late-Pleistocene to middle-Holocene soils throughout the area. Preservation of these older soils on the landscape, then, is dictated by local topography.

Determining a topographic threshold, as revealed in this study, is useful for quantifying the effects of the landscape on the preservation and distribution of buried soils and archaeological sites. Results of this study, may be comparable to other regions with plateaus and steep escarpment breaks like the Southern High Plains. Most researchers examining the effects of topographic thresholds along escarpments, however, have focused on identifying the initiation and rate of gully erosion within these regions [51–54]. Identifying the effects of a topographic threshold on the distribution and preservation of buried soils in these regions will also be important for developing research and preservation strategies to study and protect associated archaeological sites.

5. Conclusions

Current research has found a soil topographic threshold at ~810 m elevation and a change in the behavior of the South Fork that determines the amount of lateral migration of the South Fork. That change in behavior most likely is caused by the underlying geology and slope. The increased migration of the South Fork below the ~810 m elevation threshold has eroded away the late-Pleistocene to middle-Holocene terraces and their UU and ULS soils. In contrast, above the ~810 m elevation threshold, these terraces and soils are still intact due to the limited lateral migration within the upper reaches of the South Fork drainage. These areas along the escarpment breaks, then, are a good place to find intact archaeological sites dating to the late Pleistocene through middle Holocene.

The understanding of these spatial and temporal patterns, and processes controlling erosion, is particularly significant in assessing site formation and preservation within semi-arid regions.

The determination of soil thresholds, and particularly topographic threshold, that relates the preservation of buried soils and landforms provides a better understanding of the geographic distribution of the geoarchaeological record. Isolating the parent materials in this study that contributed to the formation of landforms over different time periods has allowed for independent viewing of the topographic influences on landscape preservation. This study provides the foundation or first step towards quantifying erosion and examining any potential geomorphic biases through identification of a soil topographic threshold in this highly modified area.

Author Contributions: Investigation, methodology, and writing—original draft preparation, T.C. Investigation, methodology, supervision, visualization, and writing—editing, S.H. Funding acquisition, investigation, methodology, project administration, resources, supervision, and writing—review and editing, E.J. All authors have read and agreed to the published version of the manuscript.

Funding: This research was funded by the Museum of Texas Tech University and a private foundation. This research received no external funding.

Acknowledgments: The senior author thanks David Weindorf and Richard Zartman (Plant and Soil Science, Texas Tech University) for providing guidance in this research. Thanks also are due to Doug Cunningham (Lubbock Lake Landmark), Vance Holliday (University of Arizona), Susan Casby-Horton (Plant and Soil Science, Texas Tech University), Tom Lehman (Geosciences, Texas Tech University, and Wayne Hudnall and B.L. Allen (formerly Plant and Soil Science, Texas Tech University) for their roles in this research endeavor. Thanks to Katherine Ehlers and Keith SoRelle (formerly Museum of Texas Tech University) for providing field assistance in documenting soil profiles and compiling radiocarbon dates. The authors thank the landowners for graciously allowing us access to the ranch. The authors also thank three anonymous reviewers whose suggestions improved the quality of this manuscript. This study represents part of the ongoing Lubbock Lake Landmark regional research into late-Quaternary landscape development and climatic and ecological change on the Southern Plains.

Conflicts of Interest: The authors declare no conflict of interest.

Appendix A

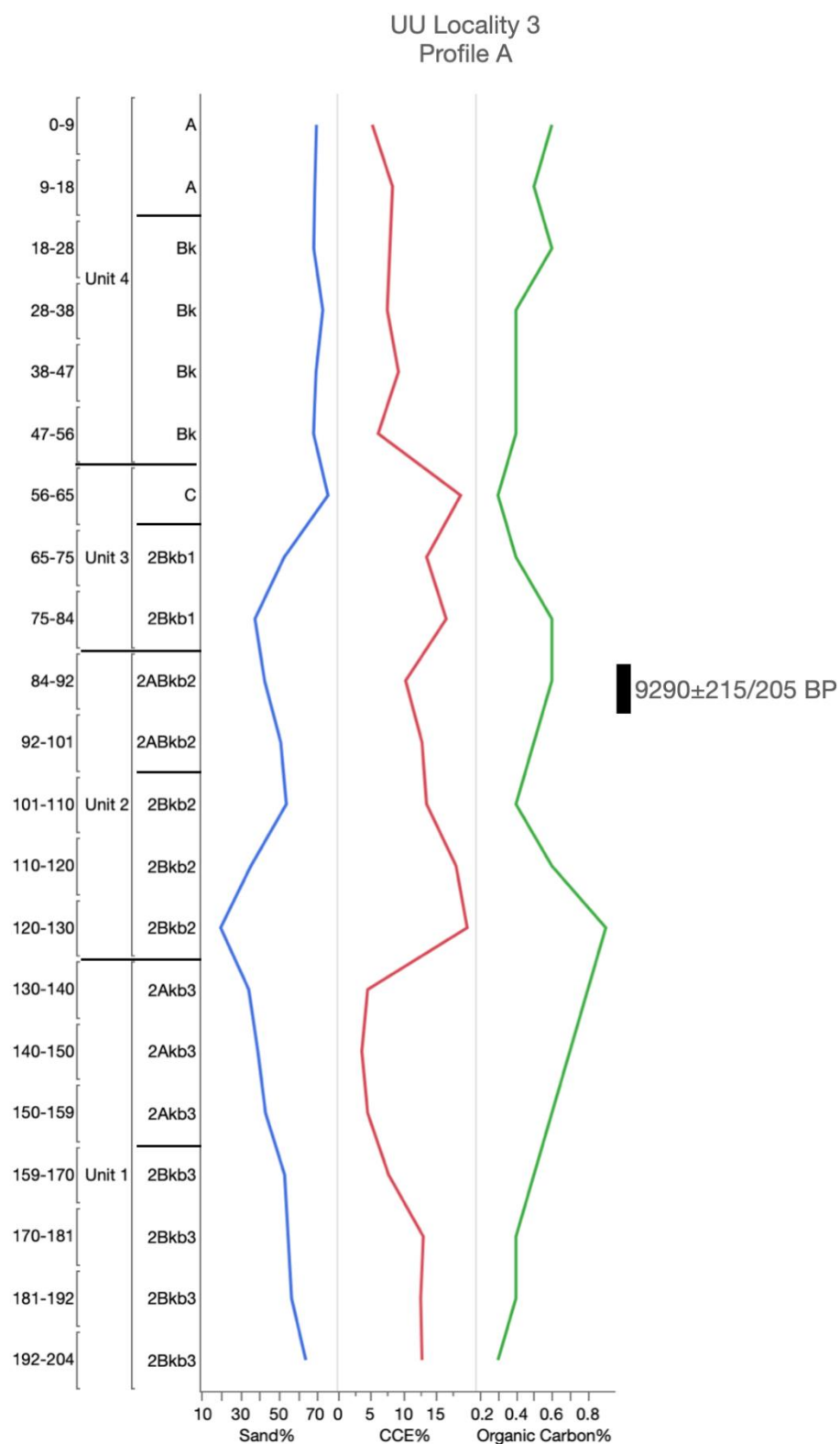


Figure A1. Accepted radiocarbon ages and soil and sediment analysis at UU Locality 3, Profile A—Post research area, northwest, Texas. CCE = calcium carbonate equivalence.

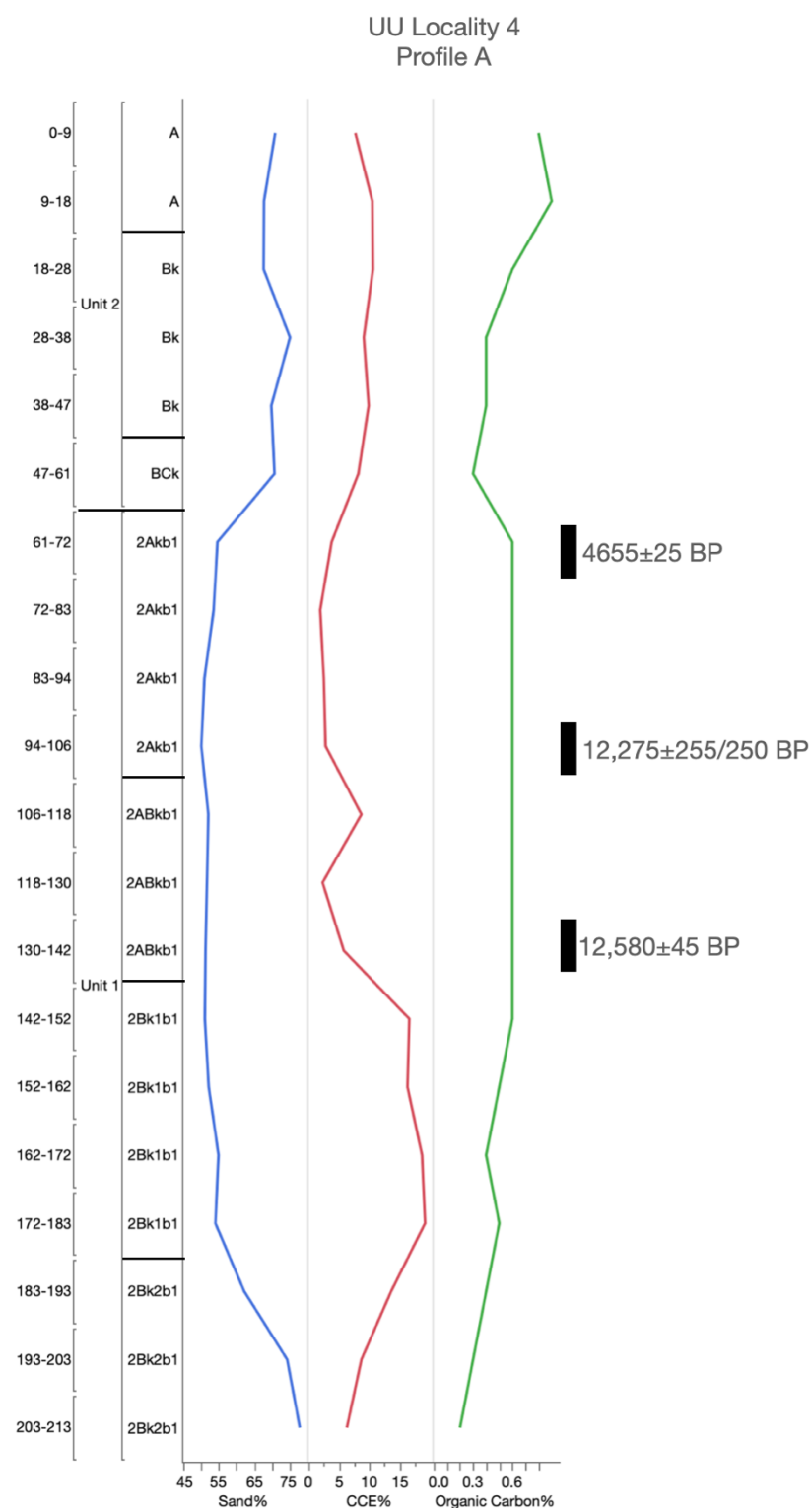


Figure A2. Accepted radiocarbon ages and soil and sediment analysis at UU Locality 4, Profile A—Post research area, northwest, Texas. CCE = calcium carbonate equivalence.

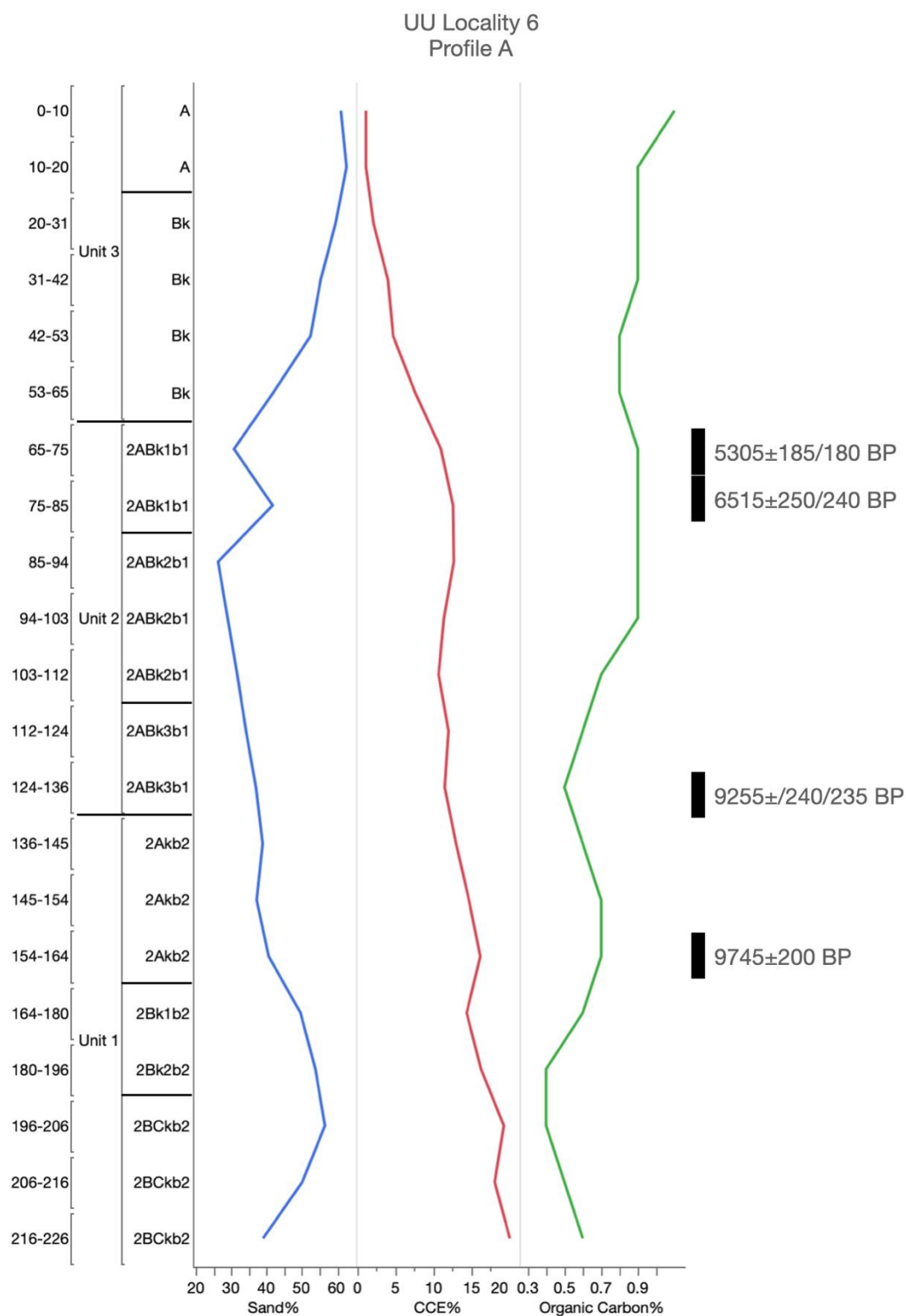


Figure A3. Accepted radiocarbon ages and soil and sediment analysis at UU Locality 6, Profile A—Post research area, northwest, Texas. CCE = calcium carbonate equivalence.

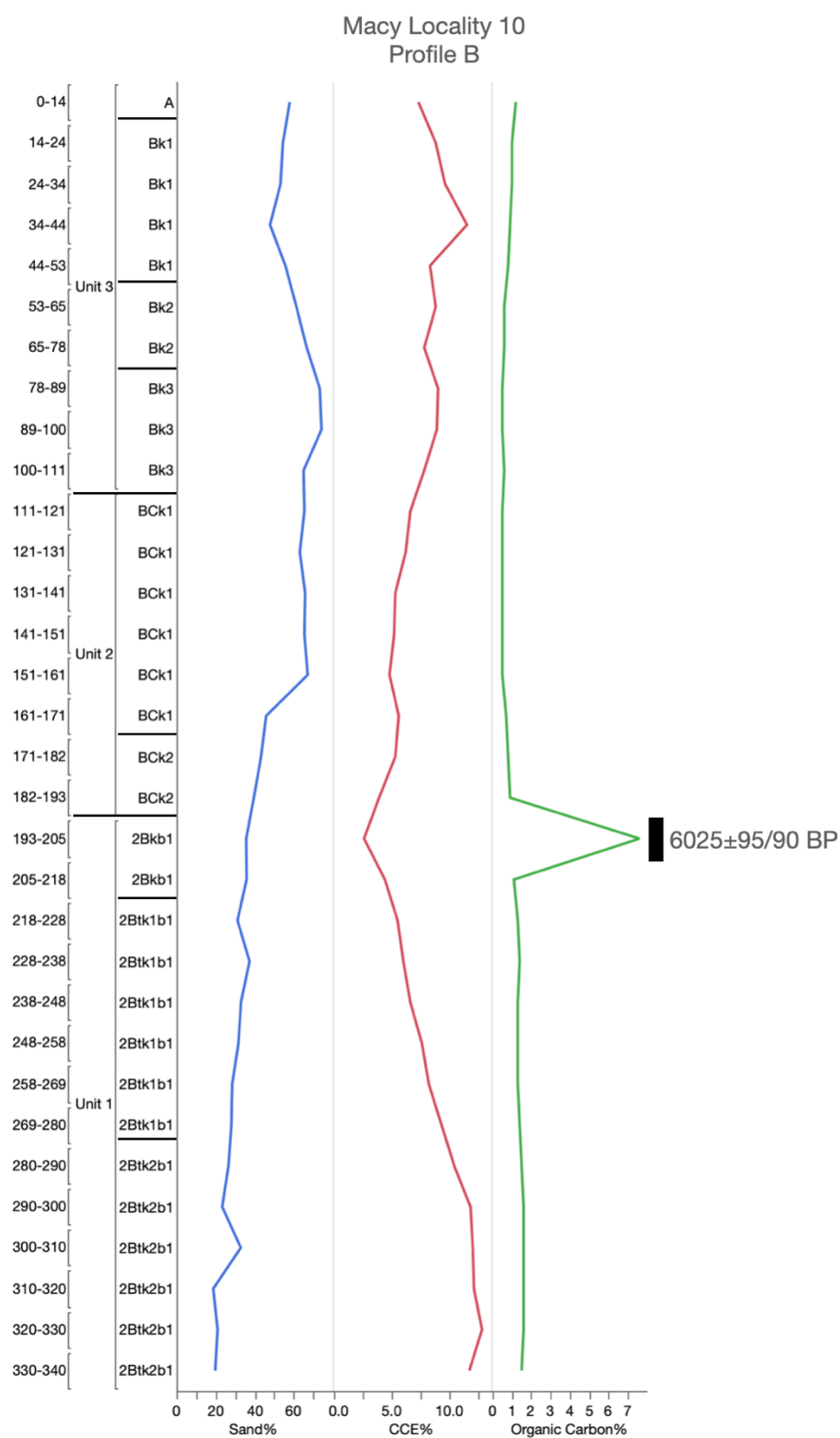


Figure A4. Accepted radiocarbon ages and soil and sediment analysis at Macy Locality 10, Profile B—Post research area, northwest, Texas. CCE = calcium carbonate equivalence.

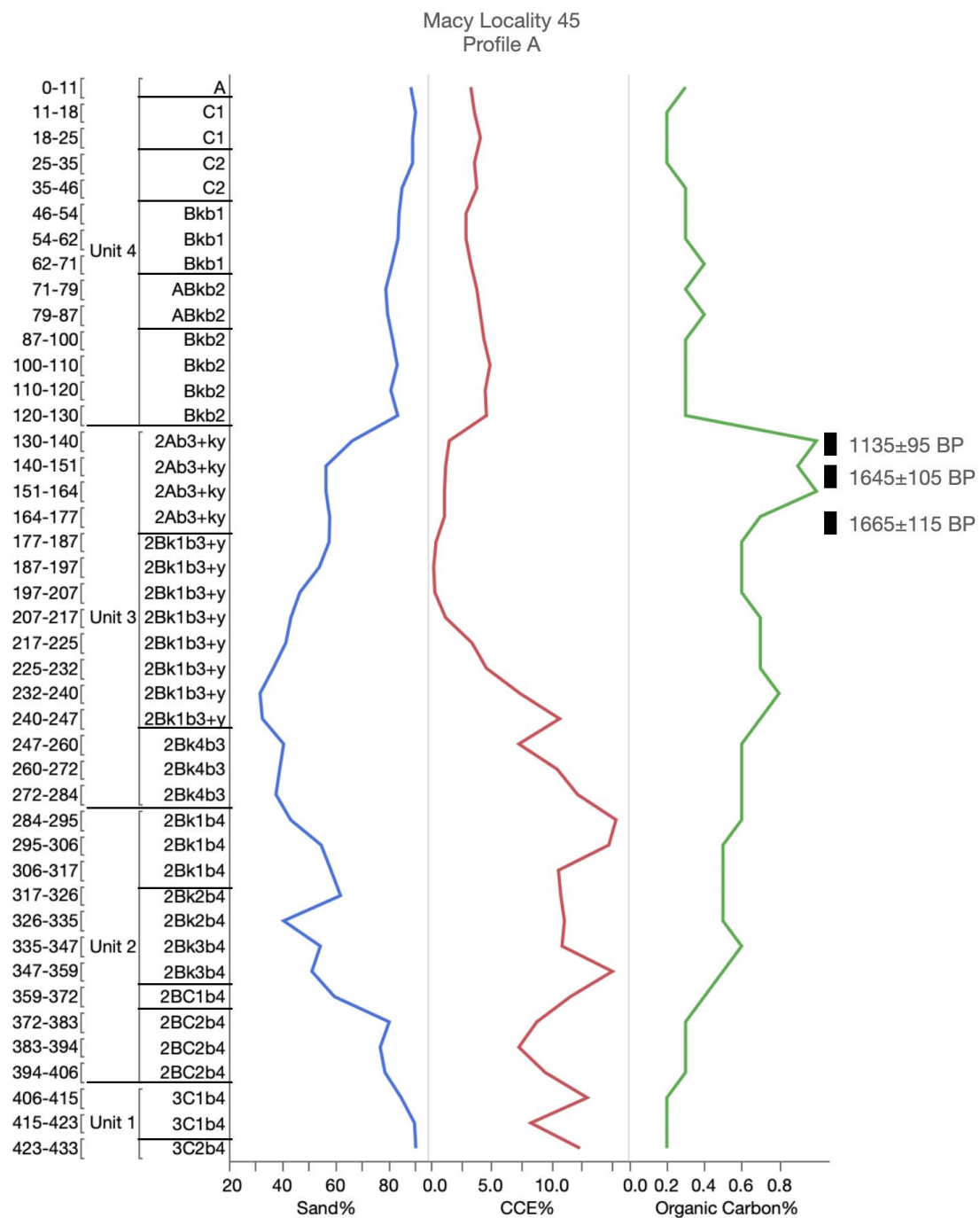


Figure A5. Accepted radiocarbon ages and soil and sediment analysis at Macy Locality 45, Profile A—Post research area, northwest, Texas. CCE = calcium carbonate equivalence.

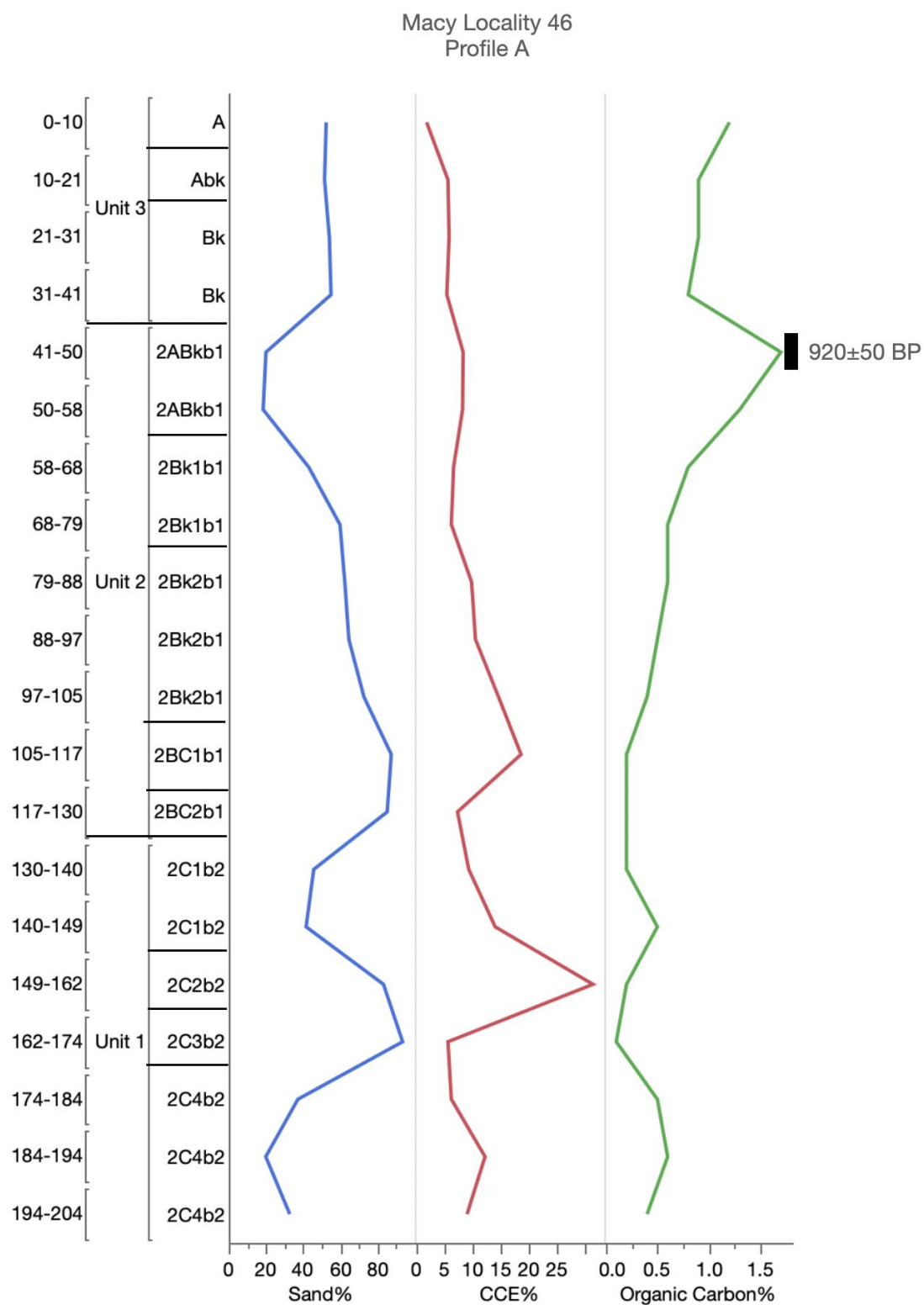


Figure A6. Accepted radiocarbon ages and soil and sediment analysis at Macy Locality 46, Profile A—Post research area, northwest, Texas. CCE = calcium carbonate equivalence.

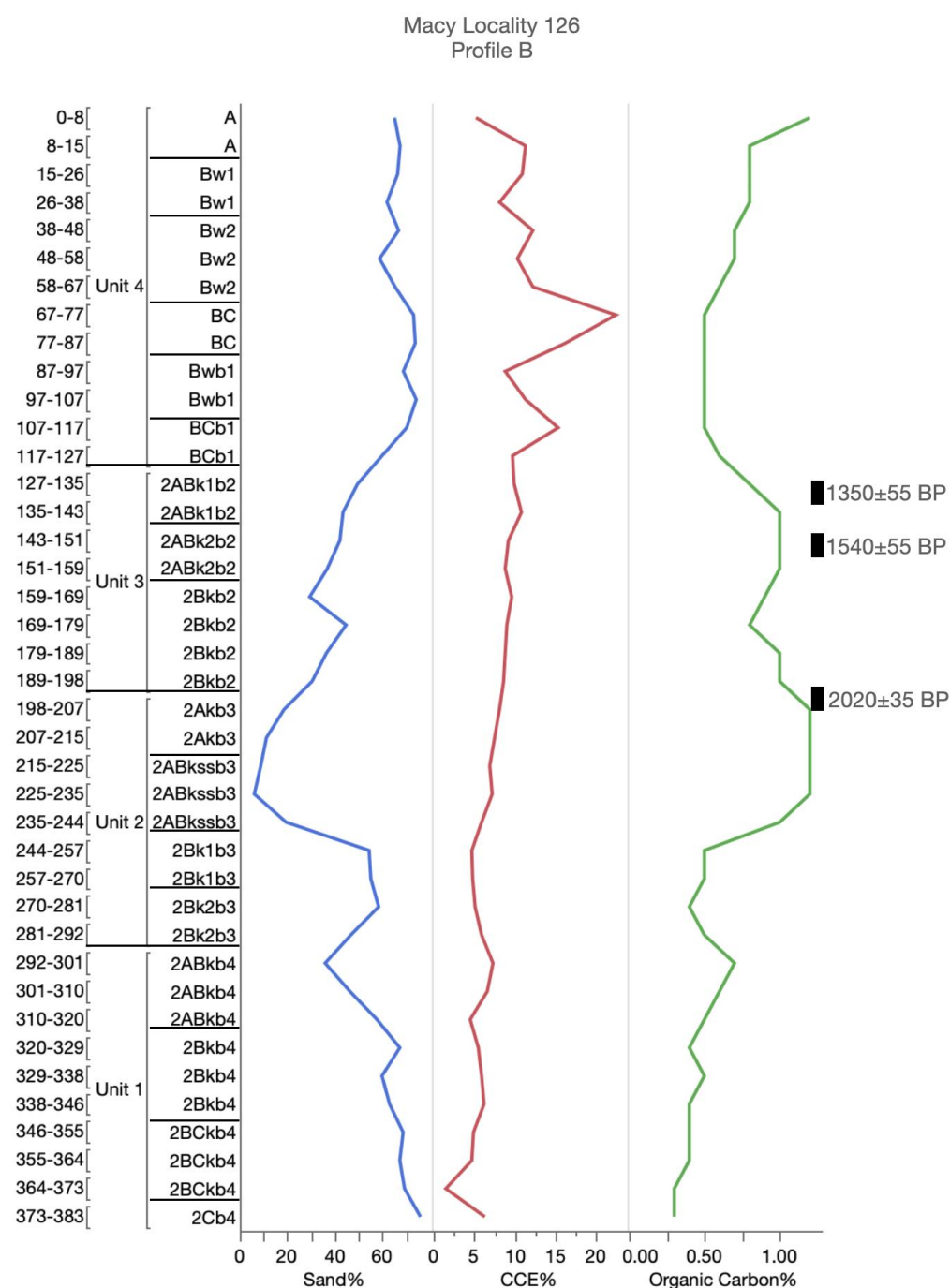


Figure A7. Accepted radiocarbon ages and soil and sediment analysis at Macy Locality 126, Profile B—Post research area, northwest, Texas. CCE = calcium carbonate equivalence.

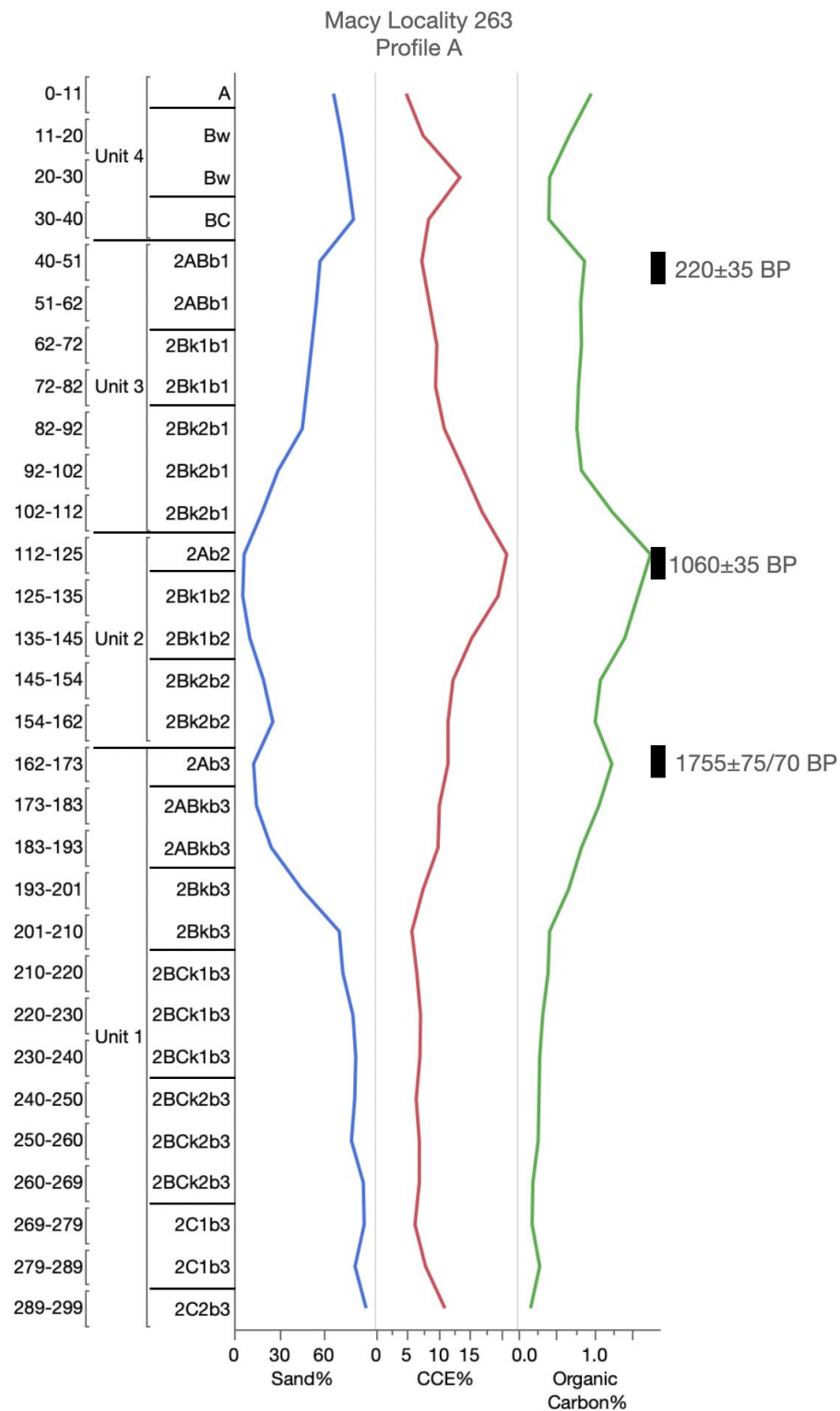


Figure A8. Accepted radiocarbon ages and soil and sediment analysis at Macy Locality 263, Profile A—Post research area, northwest, Texas. CCE = calcium carbonate equivalence.

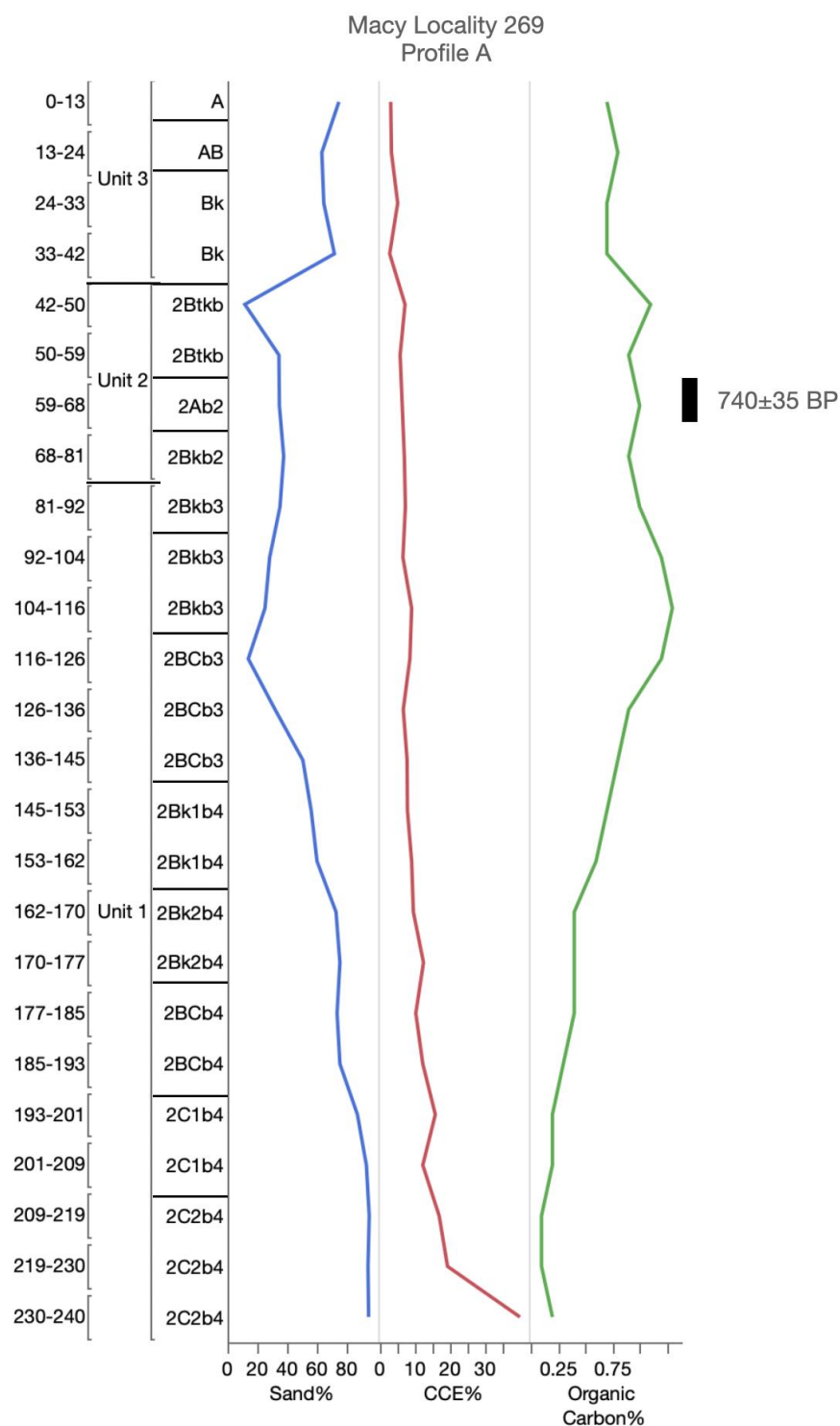


Figure A9. Accepted radiocarbon ages and soil and sediment analysis at Macy Locality 269, Profile A—Post research area, northwest, Texas. CCE = calcium carbonate equivalence.

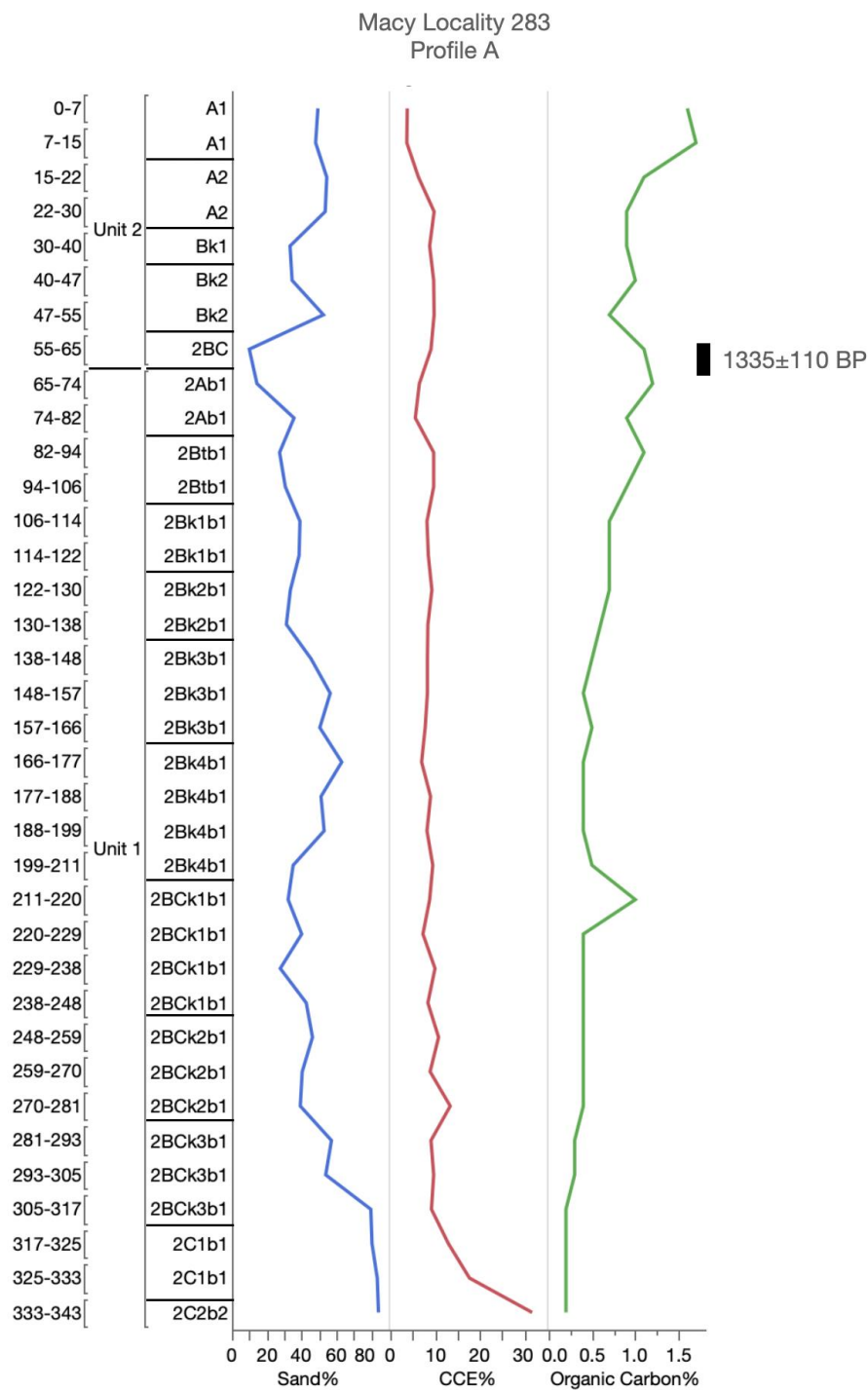


Figure A10. Accepted radiocarbon ages and soil and sediment analysis at Macy Locality 283, Profile A—Post research area, northwest, Texas. CCE = calcium carbonate equivalence.

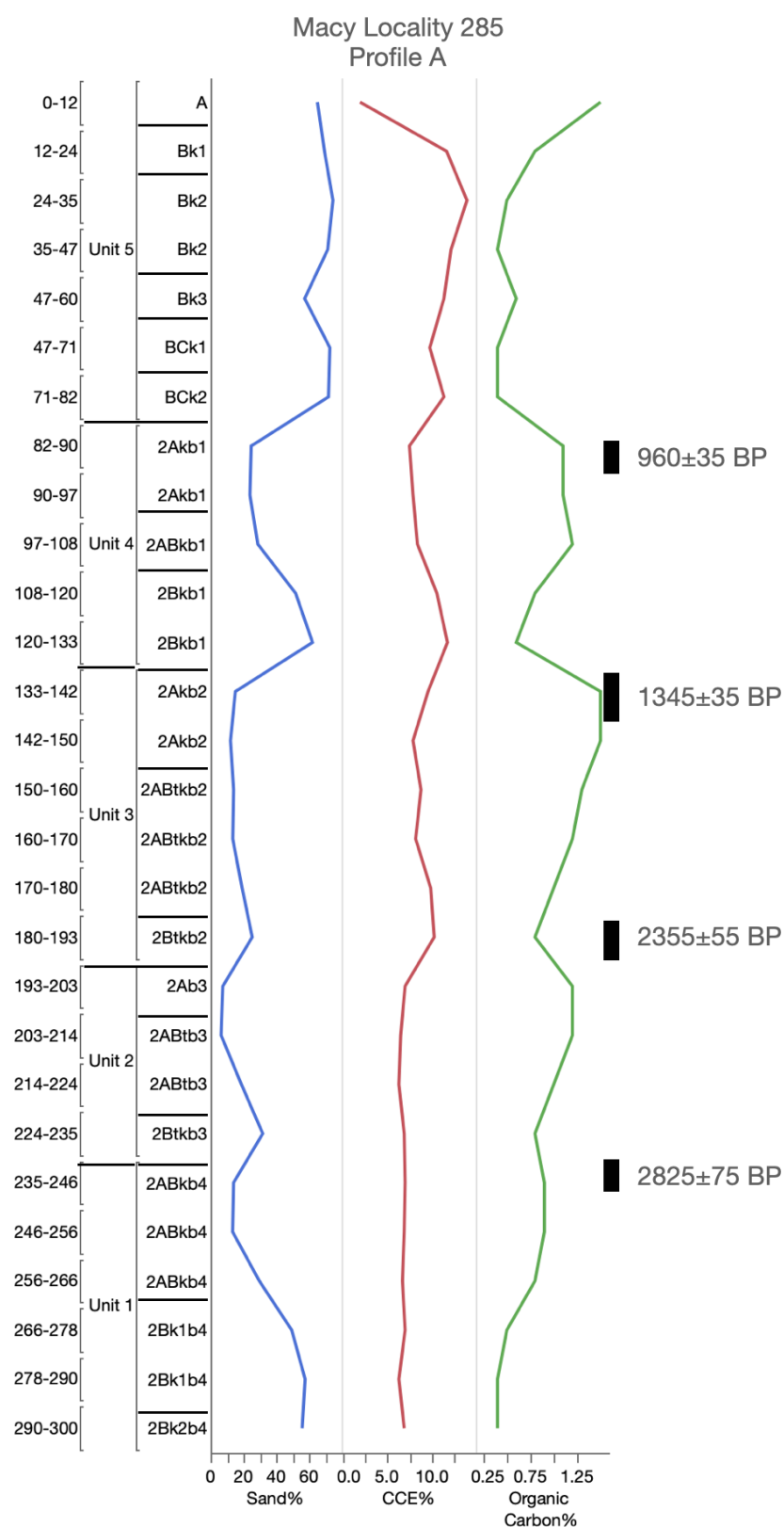


Figure A11. Accepted radiocarbon ages and soil and sediment analysis at Macy Locality 285, Profile A—Post research area, northwest, Texas. CCE = calcium carbonate equivalence.

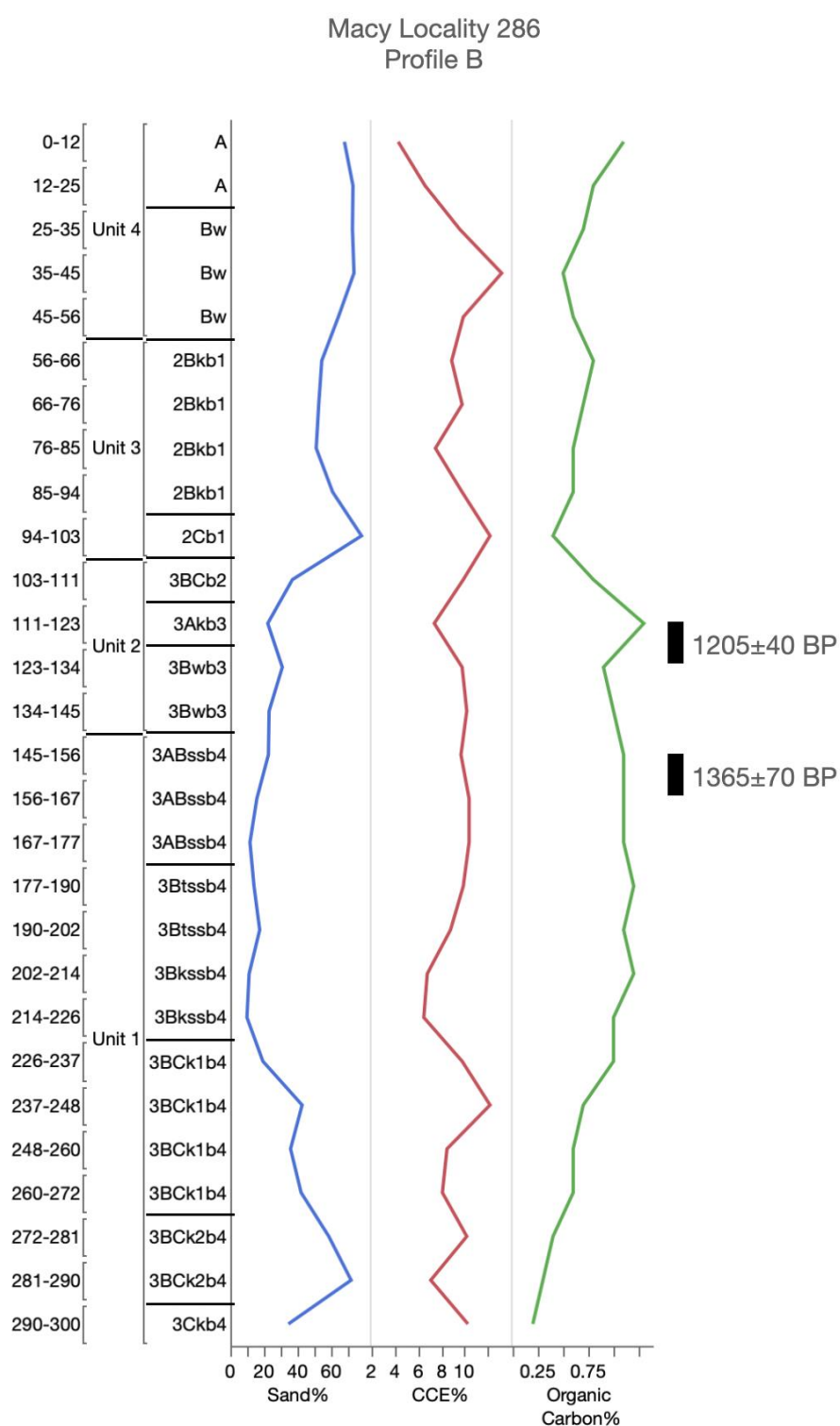


Figure A12. Accepted radiocarbon ages and soil and sediment analysis at Macy Locality 286, Profile B—Post research area, northwest, Texas. CCE = calcium carbonate equivalence.

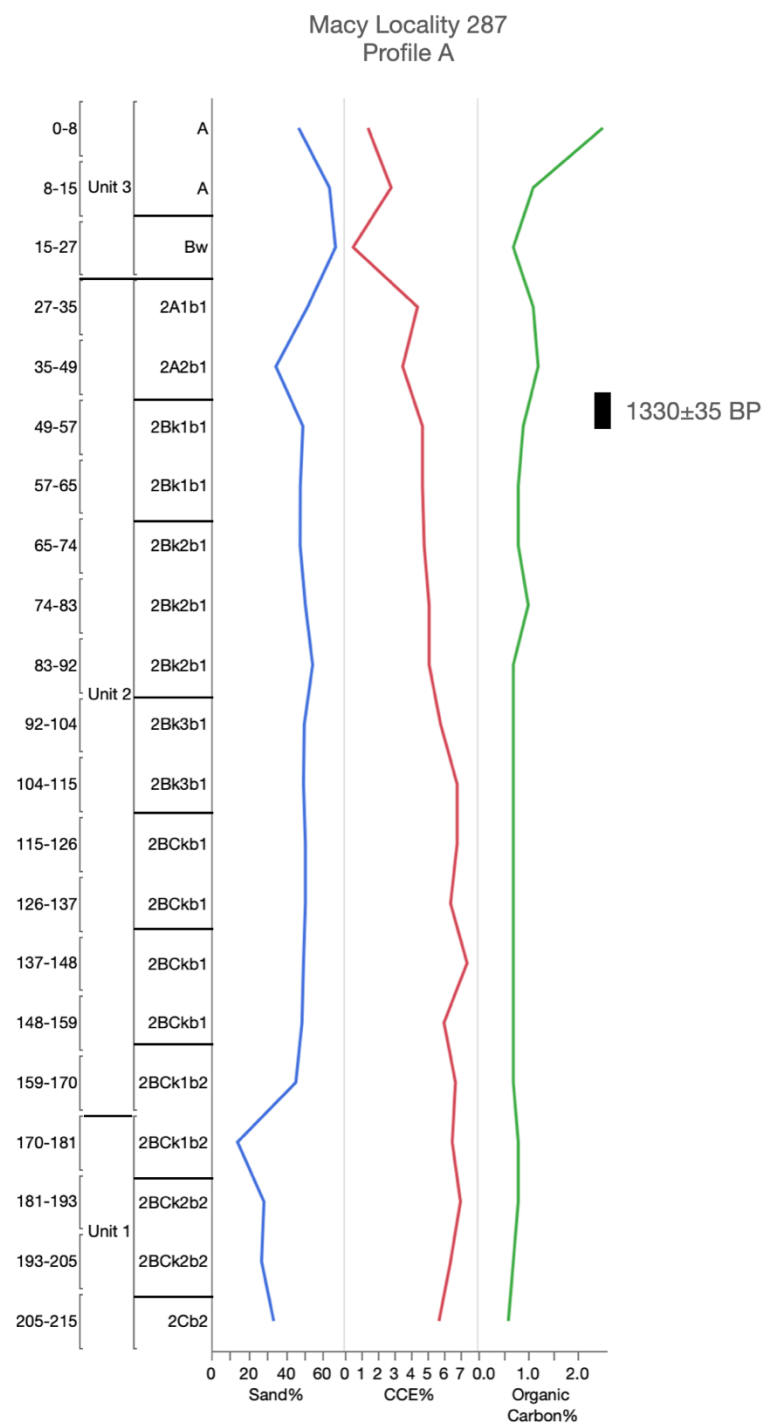


Figure A13. Accepted radiocarbon ages and soil and sediment analysis at Macy Locality 287, Profile A—Post research area, northwest, Texas. CCE = calcium carbonate equivalence.

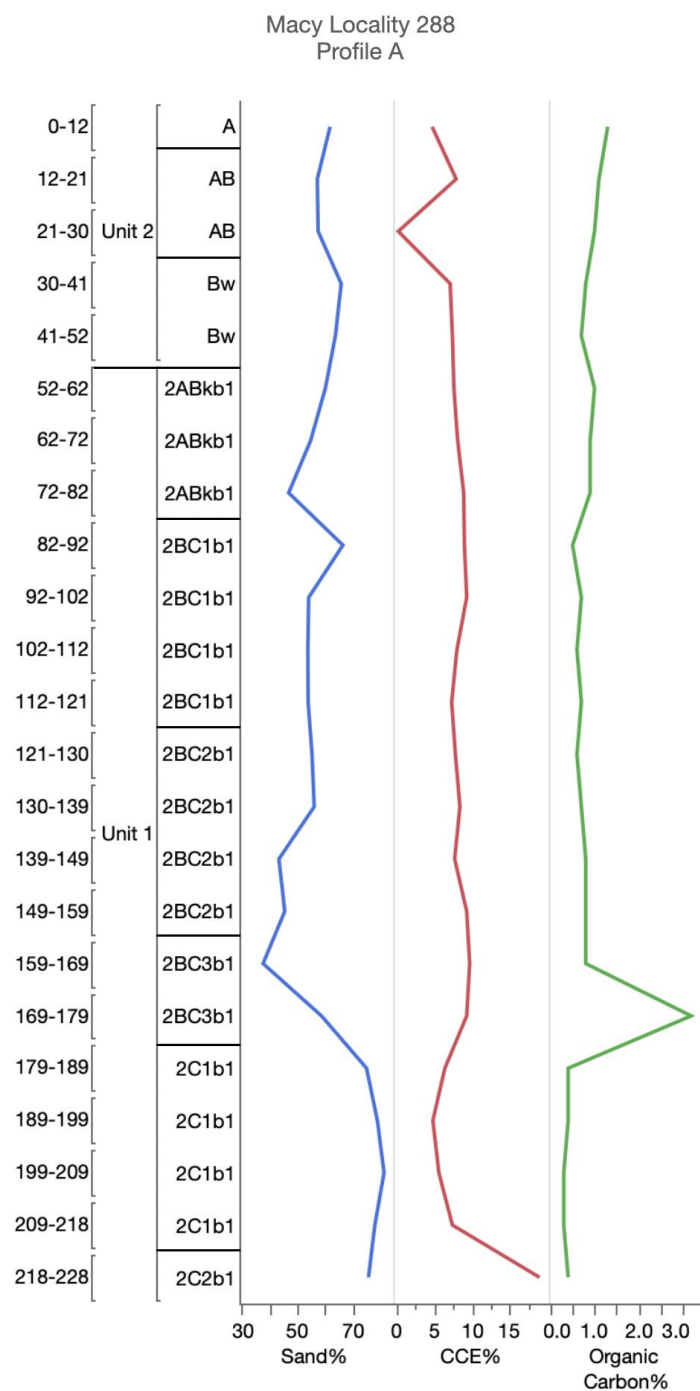


Figure A14. Accepted radiocarbon ages and soil and sediment analysis at Macy Locality 288, Profile A—Post research area, northwest, Texas. CCE = calcium carbonate equivalence.

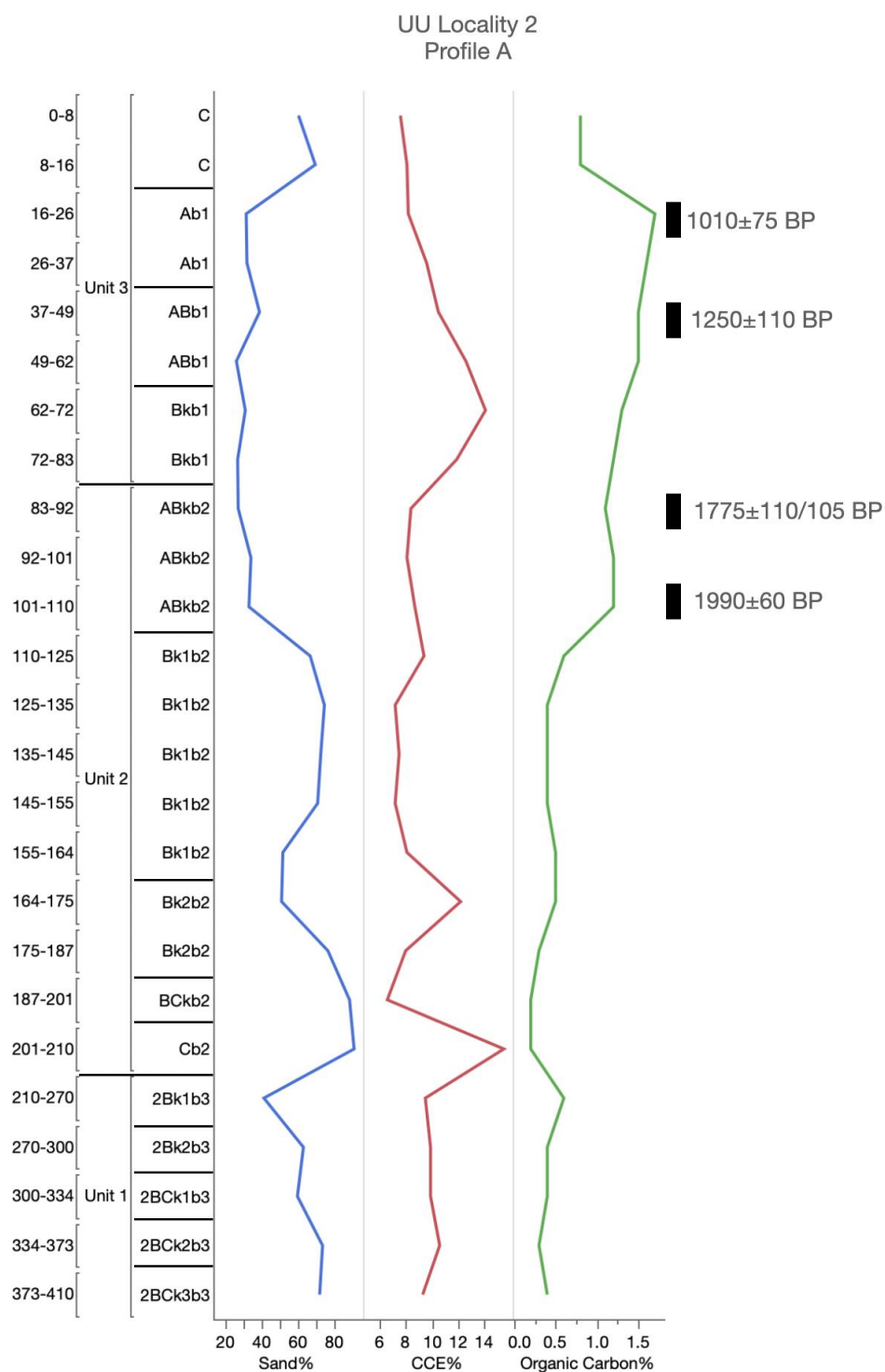


Figure A15. Accepted radiocarbon ages and soil and sediment analysis at UU Locality 2, Profile A—Post research area, northwest, Texas. CCE = calcium carbonate equivalence.

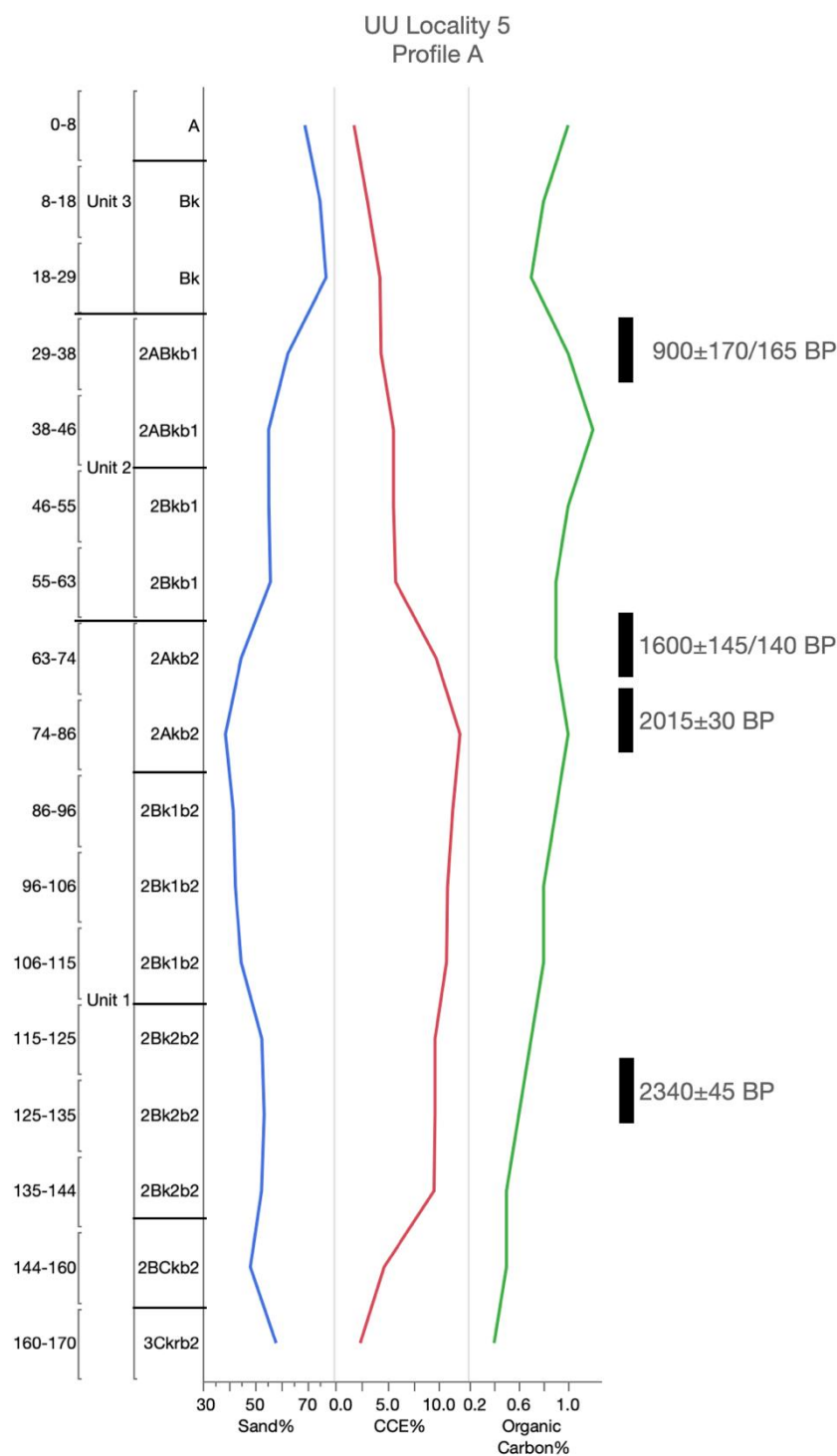


Figure A16. Accepted radiocarbon ages and soil and sediment analysis at UU Locality 5, Profile A—Post research area, northwest, Texas. CCE = calcium carbonate equivalence.

References

1. Dietrich, W.E.; Wilson, C.J.; Montgomery, D.R.; McKean, J.; Bauer, R. Erosion Thresholds and Land Surface Morphology. *Geology* **1992**, *20*, 675–679. [[CrossRef](#)]
2. McNamara, J.P.; Ziegler, A.D.; Wood, S.H. Channel Head Locations with Respect to Geomorphologic Thresholds Derived from a Digital Elevation Model: A Case Study in Northern Thailand. *For. Ecol. Manag.* **2006**, *224*, 147–156. [[CrossRef](#)]

3. Phillips, J.D. Thresholds, Mode Switching, and Emergent Equilibrium in Geomorphic Systems. *Earth Surf. Process. Landf.* **2014**, *39*, 71–79. [\[CrossRef\]](#)
4. Maignard, A.; Dyck, S.V.; Bielders, C. Assessing the Regional and Temporal Variability of the Topographic Threshold for Ephemeral Gully Initiation using Quantile Regression in Wallonia (Belgium). *Geomorphology* **2014**, *206*, 165–177. [\[CrossRef\]](#)
5. Dietrich, W.E.; Wilson, C.J.; Montgomery, D.R.; McKean, J. Analysis of Erosion Thresholds, Channel Networks, and Landscape Morphology using a Digital Terrain Model. *J. Geol.* **1993**, *101*, 259–278. [\[CrossRef\]](#)
6. Bryan, R.B. Soil Erodibility and Processes of Water Erosion on Hillslope. *Geomorphology* **2000**, *32*, 385–415. [\[CrossRef\]](#)
7. Prosser, I.P.; Abernethy, B. Predicting the Topographic Limits to a Gully Network Using a Digital Terrain Model and Process Thresholds. *Water Resour. Res.* **1996**, *32*, 2289–2298. [\[CrossRef\]](#)
8. Samani, A.; Ahmadi, H.; Jafari, M.; Boggs, G. Geomorphic Threshold Conditions for Gully Erosion in Southwestern Iran (Boushehr-Samal Watershed). *J. Asian Earth Sci.* **2009**, *35*, 180–189. [\[CrossRef\]](#)
9. Svoray, T.; Michailov, E.; Cohen, A.; Rokah, L.; Sturm, A. Predicting Gully Initiation: Comparing Data Mining Techniques, Analytical Hierarchy Processes and the Topographic Threshold. *Earth Surf. Process. Landf.* **2012**, *37*, 607–619. [\[CrossRef\]](#)
10. Fox, D.M.; Bryan, R.B. The Relationship of Soil Loss by Interrill Erosion to Slope Gradient. *Catena* **2000**, *38*, 211–222. [\[CrossRef\]](#)
11. Knapen, A.; Poesen, J. Soil Erosion Resistance Effects on Rill and Gully Initiation Points and Dimensions. *Earth Surf. Process. Landf. J. Br. Geomorphol. Res. Group* **2010**, *35*, 217–228. [\[CrossRef\]](#)
12. Poesen, J.; Torri, D.; Vanwalleghe, T. Gully Erosion: Procedures to Adopt when Modelling Soil Erosion in Landscapes Affected by Gullying. *Handb. Eros. Model.* **2011**, 360–386. [\[CrossRef\]](#)
13. Buol, S.W.; Hole, F.D.; McCracken, R.J.; Southard, R.J. *Soil Genesis and Classification*, 4th ed.; Iowa State University Press: Ames, IA, USA, 1997.
14. Holliday, V.T. *Soils in Archaeological Research*; Oxford University Press: Oxford, UK, 2004.
15. Arauza, H.M.; Simms, A.R.; Bement, L.C.; Carter, B.J.; Conley, T.O.; Woldergauy, A.; Johnson, W.C.; Jaiswal, P. Geomorphic and Sedimentary Responses of the Bull Creek Valley (Southern High Plains, USA) to Pleistocene and Holocene Environmental Change. *Quat. Res.* **2016**, *85*, 118–132. [\[CrossRef\]](#)
16. Mandel, R.D. Buried Paleoindian-age Landscapes in Stream Valleys of the Central Plains, USA. *Geomorphology* **2008**, *101*, 342–361. [\[CrossRef\]](#)
17. Schumm, S.A. Geomorphic Thresholds: The Concept and its Applications. *Trans. Inst. Br. Geogr.* **1979**, *4*, 485–515. [\[CrossRef\]](#)
18. Muhs, D.R. Intrinsic Thresholds in Soil Systems. *Phys. Geogr.* **1984**, *5*, 99–110. [\[CrossRef\]](#)
19. Jenny, H. *Factors of Soil Formation*; McGraw-Hill: New York, NY, USA, 1941.
20. Birkeland, P.W. *Soils and Geomorphology*, 3rd ed.; Oxford University Press: New York, NY, USA, 1999.
21. Butler, B.E. A New System for Soil Studies. *J. Soil Sci.* **1982**, *33*, 581–595. [\[CrossRef\]](#)
22. Murphy, L.; Hurst, S.; Holliday, V.; Johnson, E. Late Quaternary Landscape Evolution, Soil Stratigraphy, and Geoarchaeology of the Caprock Canyonlands, Northwest Texas, USA. *Quat. Int.* **2014**, *342*, 57–72. [\[CrossRef\]](#)
23. Sabin, T.J.; Holliday, V.T. Playas and Lunettes on the Southern High Plains: Morphometric and Spatial Relationships. *Ann. Assoc. Am. Geogr.* **1995**, *85*, 286–305. [\[CrossRef\]](#)
24. Lehman, T.; Chatterjee, S. Depositional Setting and Vertebrate Biostratigraphy of the Triassic Dockum Group of Texas. *J. Earth Syst. Sci.* **2005**, *114*, 325–351. [\[CrossRef\]](#)
25. Gustavson, T.C.; Baumgardner, R.W., Jr.; Caran, S.C.; Holliday, V.T.; Mehnert, H.H.; O'Neill, J.M. Quaternary Geology of the Southern Great Plains and an Adjacent Segment of the Rolling Plains. In *Quaternary Nonglacial Geology: Conterminous U.S. Centennial Volume K-2*; Geological Society of America: Boulder, CO, USA, 1991; pp. 477–501.
26. Gustavson, T.C.; Winkler, D.A. Depositional Facies of the Miocene-Pliocene Ogallala Formation, Northwestern Texas and Eastern New Mexico. *Geology* **1988**, *16*, 203–206. [\[CrossRef\]](#)
27. Ferring, C.R. Archaeological Geology of the Southern Plains. In *Archaeological Geology of North America*; Lasca, N.P., Donahue, J., Eds.; Geological Society of America: Boulder, CO, USA, 1990; pp. 253–266.
28. Bomar, G.W. *Texas Weather*; University of Texas Press: Austin, TX, USA, 1995.

29. Harragan, D. *Blue Northerners to Sea Breezes: Texas Weather and Climate*; Hendrick Long Publishing Co.: Dallas, TX, USA, 1983.
30. Brune, G. *Springs of Texas*; Branch-Smith: Fort Worth, TX, USA, 1981.
31. Soil Survey Staff. *Soil Survey Laboratory Information Manual. Soil Survey Investigations (Report 45)*; U.S. Department of Agriculture, Natural Resources Conservation Service, National Soil Survey Center: Lincoln, NE, USA, 1995.
32. Soil Survey Staff. *Soil Taxonomy (Agricultural Handbook 436)*; U.S. Department of Agriculture, Natural Resources Conservation Service: Washington, DC, USA, 1999.
33. Soil Survey Staff. *Kellogg Soil Survey Laboratory Methods Manual (Soil Survey Investigations Report 42)*; U.S. Department of Agriculture, Natural Resources Conservation Service, National Soil Survey Center: Lincoln, NE, USA, 2014.
34. Clark, C.W.; Hudnall, W.H. Field Method for Determining Carbonate. In Proceedings of the 2006 Soil Science Society of America Conference, Indianapolis, IN, USA, 12–16 November 2006.
35. Holliday, V.T. *Stratigraphy and Paleoenvironments of Late Quaternary Valley Fills on the Southern High Plains (Memoir 186)*; Geological Society of America: Boulder, CO, USA, 1995.
36. Johnson, E.; Holliday, V.T.; Martínez, G.; Gutiérrez, M.; Politis, G. Geochronology and Landscape Development along the Middle Río Quequén Grande at the Paso Otero Locality, Pampa Interserrana, Argentina. *Geoarchaeology* **2012**, *27*, 300–323. [[CrossRef](#)]
37. Hammond, A.; Goh, K.; Tonkin, P.; Manning, M.R. Chemical Pretreatments for Improving the Radiocarbon Dates of Peats and Organic Silts in a Gley Podzol Environment: Grahams Terrace, North Westland. *N. Z. J. Geol. Phys.* **1991**, *34*, 191–194. [[CrossRef](#)]
38. Head, M.; Zhou, W.; Zhou, M. Evaluation of ^{14}C Ages of Organic Fractions of Paleosols from Loess-Paleosol Sequences Near Xian, China. *Radiocarbon* **1989**, *31*, 680–695. [[CrossRef](#)]
39. Wang, Y.; Amundson, R.; Trumbore, S. Radiocarbon Dating of Soil Organic Matter. *Quat. Res.* **1996**, *45*, 282–288. [[CrossRef](#)]
40. De Reu, J.; Bourgeois, J.; Bats, M.; Zwertvaegher, A.; Gelorini, V.; De Smedt, P.; Chu, W.; Antrop, M.; De Maeyer, P.; Finke, P. Application of the Topographic Position Index to Heterogeneous Landscapes. *Geomorphology* **2013**, *186*, 39–49. [[CrossRef](#)]
41. De Reu, J.; Bourgeois, J.; De Smedt, P.; Zwertvaegher, A.; Antrop, M.; Bats, M.; De Maeyer, P.; Finke, P.; Van Meirvenne, M.; Verniers, J. Measuring the relative topographic position of archaeological sites in the landscape, a case study on the Bronze Age barrows in northwest Belgium. *J. Archaeol. Sci.* **2011**, *38*, 3435–3446. [[CrossRef](#)]
42. Weiss, A. Topographic Position and Landforms Analysis. In Proceedings of the 2001 ESRI User Conference, San Diego, CA, USA, 9–13 July 2001.
43. Conley, T.O. Paleo-Environmental Landscape Evolution on the Eastern Caprock Escarpment of the Southern High Plains, Texas. Ph.D. Thesis, Department of Geosciences, Texas Tech University, Lubbock, TX, USA, 2016.
44. Blum, M.D.; Abbott, J.T.; Valastro, S., Jr. Evolution of Landscapes on the Double Mountain Fork of the Brazos River, West Texas: Implications for Preservation and Visibility of the Archaeological Record. *Geoarchaeology* **1992**, *7*, 339–370. [[CrossRef](#)]
45. Church, M. Geomorphic Thresholds in Riverine Landscapes. *Freshw. Biol.* **2002**, *47*, 541–557. [[CrossRef](#)]
46. Ehlers, K.B.; Moe, J.R.; Johnson, E.; Hurst, S. Trade on the Llano Estacado: A Protohistoric Site (41GR793) at the Base of the Southern High Plains, Texas. In Proceedings of the 69th Plains Anthropological Conference, Tucson, AZ, USA, 26–29 October 2011.
47. Hurst, S.; Ward, D.C.; Johnson, E.; Cunningham, D. Cowboy Life along the Llano Estacado Eastern Escarpment of Northwest Texas: Insights from Macy Locality 16 (41GR722). *Hist. Archaeol.* **2018**, *52*, 332–347. [[CrossRef](#)]
48. Moretti, J.; Johnson, E. The First Record of the Jumping Mouse *Zapus* from the Southern High Plains. *PaleoAmerica* **2015**, *1*, 121–123. [[CrossRef](#)]
49. Moretti, J.A. The Vertebrate Fauna of Macy Locality 100: Exploring Late Pleistocene Community Composition in Non-Analog North America. Master's Thesis, Interdisciplinary Studies, Texas Tech University, Lubbock, TX, USA, 2018.
50. Hurst, S.; Johnson, E.; Cunningham, D. Macy Locality-15, a Late-Paleoindian Site along the Caprock Escarpment of Texas. *Curr. Res. Pleistocene* **2008**, *25*, 68–69.

51. Hall, S.A. Channel Trenching and Climatic Change in the Southern US Great Plains. *Geology* **1990**, *18*, 342–345. [[CrossRef](#)]
52. Cama, M.; Schillaci, C.; Kropáček, J.; Hochschild, V.; Bosino, A.; Märker, M. A Probabilistic Assessment of Soil Erosion Susceptibility in a Head Catchment of the Jemma Basin, Ethiopian Highlands. *Geosciences* **2020**, *10*, 248. [[CrossRef](#)]
53. Hancock, G.R.; Evans, K.G. Gully Position, Characteristics and Geomorphic Thresholds in an Undisturbed Catchment in Northern Australia. *Hydrol. Process.* **2006**, *20*, 2935–2951. [[CrossRef](#)]
54. Kariminejad, N.; Rossi, M.; Hosseinalizadeh, M.; Pourghasemi, H.R.; Santosh, M. Gully Head Modelling in Iranian Loess Plateau Under Different Scenarios. *Catena* **2020**, *194*, 1047693. [[CrossRef](#)]

Publisher’s Note: MDPI stays neutral with regard to jurisdictional claims in published maps and institutional affiliations.



© 2020 by the authors. Licensee MDPI, Basel, Switzerland. This article is an open access article distributed under the terms and conditions of the Creative Commons Attribution (CC BY) license (<http://creativecommons.org/licenses/by/4.0/>).